PARASITIC DISEASES

Discovery of short-course antiwolbachial quinazolines for elimination of filarial worm infections

Malina A. Bakowski[1], Roohollah Kazem Shiroodi[1], Renhe Liu[2], Jason Olejniczak[1], Baiyuan Yang[1], Kerstin Gagaring[1], Hui Guo[1], Pamela M. White[3], Laura Chappell[3], Alain Debec[4], Frédéric Landmann[5], Bettina Dubben[6], Franziska Lenz[6], Dominique Struever[6], Alexandra Ehrens[6], Stefan J. Frohberger[6], Hanna Sjoberg[7], Nicolas Pionnier[7], Emma Murphy[7], John Archer[7], Andrew Steven[7], Valerine C. Chunda[8,9], Fanny F. Fombad[8,9], Patrick W. Chounna[8,9], Abdel J. Njouendou[8,9], Haelly M. Metuge[8], Bertrand L. Ndzeshang[8,9], Narcisse V. Gandjui[8,9], Desmond N. Akumtoh[8,9], Tayong D. B. Kwenti[8,9], Ashley K. Woods[1], Sean B. Joseph[1], Mitchell V. Hull[1], Wen Xiong[2], Kelli L. Kuhen[1], Mark J. Taylor[7], Samuel Wanji[8,9], Joseph D. Turner[7], Marc P. Hübner[6], Achim Hoerauf[6], Arnab K. Chatterjee[1], Jason Roland[1], Matt S. Tremblay[1], Peter G. Schultz[1], William Sullivan[3], Xin-Jie Chu[2], H. Michael Petrassi[1], Case W. McNamara[1]*

Parasitic filarial nematodes cause debilitating infections in people in resource-limited countries. A clinically validated approach to eliminating worms uses a 4- to 6-week course of doxycycline that targets *Wolbachia*, a bacterial endosymbiont required for worm viability and reproduction. However, the prolonged length of therapy and contraindication in children and pregnant women have slowed adoption of this treatment. Here, we describe discovery and optimization of quinazolines CBR417 and CBR490 that, with a single dose, achieve >99% elimination of *Wolbachia* in the in vivo *Litomosoides sigmodontis* filarial infection model. The efficacious quinazoline series was identified by pairing a primary cell-based high-content imaging screen with an orthogonal ex vivo validation assay to rapidly quantify *Wolbachia* elimination in *Brugia pahangi* filarial ovaries. We screened 300,368 small molecules in the primary assay and identified 288 potent and selective hits. Of 134 primary hits tested, only 23.9% were active in the worm-based validation assay, 8 of which contained a quinazoline heterocycle core. Medicinal chemistry optimization generated quinazolines with excellent pharmacokinetic profiles in mice. Potent antiwolbachial activity was confirmed in *L. sigmodontis*, *Brugia malayi*, and *Onchocerca ochengi* in vivo preclinical models of filarial disease and in vitro selectivity against *Loa loa* (a safety concern in endemic areas). The favorable efficacy and in vitro safety profiles of CBR490 and CBR417 further support these as clinical candidates for treatment of filarial infections.

INTRODUCTION

Parasitic filarial nematodes, including ones that cause lymphatic filariasis and onchocerciasis (also known as river blindness), were estimated in 2013 to infect 43.8 million and 17 million people worldwide, respectively (*1*) with more than a billion at risk of infection (*2*). Neither lymphatic filariasis nor onchocerciasis is commonly lethal; however, they are a recognized source of considerable morbidity and suffering (*3*). In addition to acute symptoms, these long-term infections often result in disfigurement and social discrimination and contribute to increased poverty of the afflicted individuals and their families. Both lymphatic filariasis and onchocerciasis are caused by long-lived filarial nematodes (roundworms) transmitted by blood-feeding insect vectors. Onchocerciasis is caused exclusively by *Onchocerca volvulus*, and lymphatic filariasis is caused mainly by *Wuchereria bancrofti* and by the closely related *Brugia* species (*Brugia malayi* and *Brugia timori*). Although the adults (macrofilariae) persist within human hosts for up to 15 years, they release thousands of microfilariae each day that either are the main cause or contribute to symptoms of disease and are also the developmental stage responsible for transmission back to the insect vector.

There is no short-course cure for these infections, and current control treatments have been centered on mass drug administration (MDA) campaigns to interrupt transmission and to alleviate symptoms for the duration of the reproductive life span of adult female parasites, variably estimated at 5 to 8 years (*4*). The recommended treatment for onchocerciasis is the drug ivermectin (Mectizan), administered at least once yearly to all at risk of infection. Ivermectin works by killing microfilariae and temporarily sterilizing, but not killing, adult worms. Current recommended treatment for lymphatic filariasis varies by geography: albendazole together with ivermectin in Africa where onchocerciasis is coendemic with lymphatic filariasis and albendazole with diethylcarbamazine in the rest of the world. These treatments likewise lead to the death of microfilariae, not the adult parasites, and these drug regimens must be maintained for at least 5 years. Although MDA of ivermectin for onchocerciasis has been ongoing for more than 25 years (*5*), there are concerns over development of drug resistance (*6*), which has already been reported in veterinary medicine (*7*, *8*); the extensive MDA coverage that must be achieved to meet elimination targets (*9*, *10*); and with overall compliance of at-risk populations (*11*, *12*). In addition, treatments with diethylcarbamazine or ivermectin are contraindicated in patients with a high load of microfilariae of the African eye worm *Loa loa*

[1]Calibr at Scripps Research, La Jolla, CA 92037, USA. [2]Global Health Drug Discovery Institute (GHDDI), Beijing, China. [3]University of California Santa Cruz, Santa Cruz, CA 95064, USA. [4]Jacques Monod Institute, University Paris Diderot/CNRS, 75013 Paris, France. [5]CRBM, University of Montpellier, CNRS, Montpellier, France. [6]Institute for Medical Microbiology, Immunology and Parasitology, University Hospital Bonn, Bonn, Germany. [7]Research Centre for Drugs and Diagnostics, Department of Parasitology, Liverpool School of Tropical Medicine, Pembroke Place, Liverpool L3 5QA, UK. [8]Research Foundation in Tropical Diseases and the Environment, Buea, Cameroon. [9]Parasite and Vector Biology Research Unit, Department of Microbiology and Parasitology, Faculty of Science, University of Buea, Buea, Cameroon.
*Corresponding author. Email: cmcnamara@scripps.edu

(>30,000 to 50,000 microfilariae/ml of blood) due to severe adverse events (*13*). Lower densities of microfilariae can also cause other, non-neurological adverse events, and overall concern over the potential for *L. loa*–associated side effects can reduce adherence to MDA campaigns (*12*).

An attractive and clinically validated strategy for developing a treatment to selectively kill adult worms is targeting the bacterial endosymbiont of onchocerciasis- and lymphatic filariasis–causing worms, *Wolbachia*, which is absent from *L. loa* nematodes. *Wolbachia* are Gram-negative obligate intracellular bacteria that are widely distributed among a variety of arthropods, where they are considered to be reproductive parasites, known for induction of parthenogenesis, feminization, and male killing (*14*). In filarial nematodes, *Wolbachia* are essential endosymbionts, needed by adult worms for both reproduction and viability. Early experiments have shown that tetracycline treatment could prevent experimental infections of rodents with *Brugia* (*15*) and *Litomosoides sigmodontis* but not with the *Wolbachia*-free species *Acanthocheilonema viteae* (*16*). The finding that *Wolbachia* is widely distributed among filarial nematodes (*17*) stimulated great interest in antibiotic antifilarial therapy (*18*). Subsequently, it has been shown in humans that treatment with doxycycline over a period of 4 to 6 weeks to eliminate *Wolbachia* from adult worms is sterilizing and eventually macrofilaricidal, with the life span of *Wolbachia*-depleted worms reduced by 70 to 80% (from ~10 years to 2 to 3 years) (*19*–*22*). An added benefit of this approach is potential reduction of inflammation because adverse inflammatory reactions to anthelmintic treatment have been associated with *Wolbachia* released in patient plasma (*23*, *24*). However, doxycycline is contraindicated for treatment of pregnant women and children under 8 years of age. The prolonged length of treatment also represents potential challenges with compliance and contributes to cost of therapy, highlighting the need for faster, safer, and more effective therapies. Here, we describe the identification of quinazolines CBR417 and CBR490 that are able to achieve very rapid clearance of *Wolbachia* from filarial nematodes in in vivo preclinical models of disease and offer the potential for development of a short-course cure to treat filarial worm infections.

RESULTS

Primary high-throughput phenotypic screen identifies compounds with specific antiwolbachial activity

Because no nematode cell lines have been established to date, to rapidly identify compounds with antiwolbachial activity, we adapted and miniaturized an in vitro high-content imaging assay, which relied on *Drosophila melanogaster* cells naturally infected with *w*Mel strain of *Wolbachia* (*25*). In the adapted assay, we used the LDW1 cell line (*26*) and two fluorescence in situ hybridization (FISH) probes specific to *Wolbachia* 16*S* ribosomal RNA (rRNA) to unambiguously stain *Wolbachia* and measure bacterial load inside host cells (Fig. 1, A to C). *Wolbachia* are sensitive to tetracycline and rifamycin antibiotics (*27*, *28*), and these controls demonstrated specific antiwolbachial activity in the assay, with doxycycline's half-maximal inhibitory concentration IC_{50} = 279 nM and rifampicin IC_{50} = 5 nM (Fig. 1D). Optimized assay conditions yielded a robust assay with Z' factors of >0.5 (table S1). Further miniaturization to 1536-well format did not reduce assay quality (Fig. 1C and Table 1). Using this optimized assay, we screened ~300,368 small molecules from established libraries, including ReFRAME (*29*), for antiwolbachial activity (table S1), with an overall hit rate of 0.70%. Reconfirmed hits were tested against *Wolbachia* in dose response and for cytotoxicity in the mammalian human embryonic kidney (HEK) 293T and HepG2 cell lines (table S1). Overall, we identified and reconfirmed 299 potent (IC_{50} < 1 μM) and selective [half-maximal cytotoxic concentration (CC_{50}):IC_{50} > 10] antiwolbachial compounds (Fig. 1, D to H, and table S1).

We identified a number of known drugs and bioactive molecules among our potent and selective hits including antibiotics, signal transduction modulators, antineoplastics, antifungals, and antivirals (Fig. 2, fig. S1, and table S2). Antibiotics made up the largest category (46%) of the identified known drugs and included tetracyclines, rifamycins, peptide deformylase inhibitors, pleuromutilins, fluoroquinolones, and aminocoumarins. Many of these displayed exquisite potencies against *Wolbachia* in vitro (e.g., coumermycin IC_{50} = 1.5 nM). Among the antiwolbachial antibiotic hits, we also identified macrolide antibiotics tylosin and its derivative tylvalosin, with *w*Mel IC_{50} values of 720 and 350 nM, respectively. However, poor bioavailability, previously identified toxicity liabilities, challenging and costly synthesis, and, most importantly, lack of retained activity against filarial *Wolbachia* made these unattractive for repurposing or further development.

We also identified a number of novel compounds among the hits. To determine whether these antiwolbachial hits were *Wolbachia*-specific and/or had antibiotic activity, we screened them against a panel of extracellular bacteria. As expected, antibiotics and known drugs showed activity against many bacterial species, but very few novel small molecules inhibited microbial growth, even at the highest concentration tested of 20 μM (Fig. 2 and table S3). This suggests that the novel chemical scaffolds identified in our screen had *Wolbachia*-specific activity or acted on a host cell process required for *Wolbachia*'s intracellular survival. Likewise, the optimized quinazoline leads CBR417 and CBR490 did not generally inhibit extracellular bacterial growth (table S4).

A worm-based ex vivo assay rapidly identifies hits with antifilarial *Wolbachia* activity

Our primary cell-based assay identified compounds with activity against *w*Mel, a strain of *Wolbachia* that infects *D. melanogaster*. Validation of antiwolbachial compound activity against filarial *Wolbachia* commonly requires in vivo models, which is not amenable to rapid compound optimization cycles and has impeded drug discovery efforts. To overcome this limitation, we developed an orthogonal ex vivo validation assay that would allow us to prioritize hits in a native context against filarial *Wolbachia* (Figs. 3 and 4A and fig. S2). On the basis of previous studies (*25*), we selected quantification of filarial *Wolbachia* stained via 16*S* rRNA FISH near a convenient landmark for quantification, the ovary distal tip cell (DTC), of *B. pahangi* to validate our primary screen hits. The *Wolbachia* distribution in the ovaries is predictable and consistent compared to the variable distribution in hypodermal chords, with highest concentrations near the DTC (Fig. 3, A to F, and figs. S2, A and B) (*30*). This population appears more refractive to compound treatment in the 3-day ex vivo assay compared to the population found in the hypodermis (Fig. 3, G and H), as has also been observed in *Onchocerca ochengi* worms in vivo (*31*). Moreover, the reproductive tract is a relevant site for antiwolbachial drug action, and clearance in germline stem cells is likely critical to prevent recrudescence of the bacteria after cessation of treatment.

Doxycycline treatment of up to 9 μM was insufficient to completely clear *w*Bp from *B. pahangi* ovaries in 3 days, but 1 and 3 μM treatments eliminated about 75% of *Wolbachia*, with an estimated EC_{50}

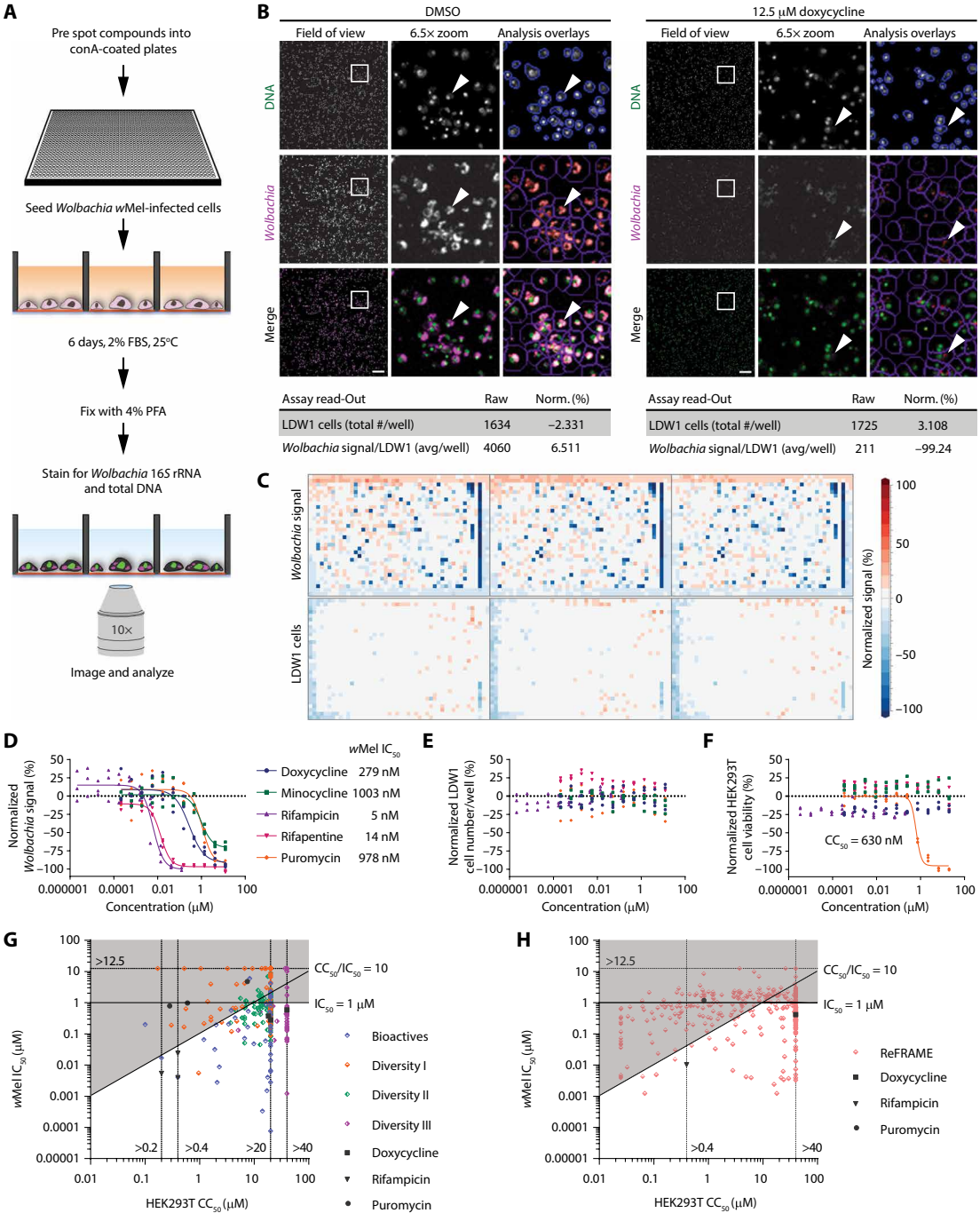

Fig. 1. A primary cell-based high-throughput phenotypic screen identifies compounds with potent and selective antiwolbachial activity. (**A**) Schematic of primary antiwolbachial screen workflow. conA, concanavalin A; PFA, paraformaldehyde; FBS, fetal bovine serum. (**B**) Representative images from dimethyl sulfoxide (DMSO)– and doxycycline-treated wells. One field of view (covering nearly the entire surface of each well) and a zoomed in segment with or without analysis overlays are shown (outline of LDW1 cell nuclei in blue, perimeter of analysis area extending beyond the nucleus in purple, and the identified *Wolbachia* spots are demarcated with a transparent red mask). In the merged image, *Wolbachia* 16*S* rRNA FISH signal is colored magenta, and DNA signal [4′,6-diamidino-2-phenylindole (DAPI)] is colored green. Raw and normalized (Norm.) values (see Materials and Methods) calculated from the images shown in (A) are listed. Scale bars, 100 μm. avg, average. (**C**) Heat map images of analysis results from plates ran in triplicate. Normalized activity values (%) for *Wolbachia* signal and cell numbers are indicated according to the scale bar. DMSO-treated wells in column 45 and individual positive control-treated wells (blocks of wells with 12.5 μM doxycycline, 0.125 μM rifampicin, or 12.5 uM puromycin) in column 46. (**D**) Eleven-point 1:3 dose-response curves of known antibiotics with activity against *Wolbachia*, including puromycin cell toxicity positive control. (**E**) LDW1 cell number dose-response data. (**F**) Mammalian HEK293T cytotoxicity dose-response data. Puromycin CC_{50} is shown. (**G**) Powder reconfirmation results for Bioactive and Diversity libraries and (**H**) the ReFRAME library, where the *w*Mel IC_{50} values of each compound are plotted against their mammalian cytotoxicity (HEK293T CC_{50} values). Compounds are color-coded on the basis of library origin. Hit potency and selectivity criteria ($IC_{50} < 1$ μM and CC_{50}:$IC_{50} > 10$) are shown as solid lines, and grayed out areas represent values that do not meet these thresholds. Dotted lines represent maximal concentrations tested in dose-response studies (e.g., 12.5 μM in the antiwolbachial primary assay).

Table 1. Structures and activities of quinazoline antiwolbachials. MW, molecular weight; n/d, not determine; EC_{50}, half-maximal effective concentration.

	Screen hit	Failed subseries lead	Successful subseries lead	Advanced leads		Optimized leads	
	CBR008	**CBR063**	**CBR422**	**CBR625**	**CBR715**	**CBR417**	**CBR490**
Subseries	Amide	Amide	Oxadiazole	Oxadiazole	Methylpyridine	Oxadiazole	Methylpyridine
	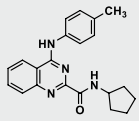	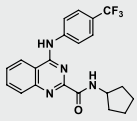	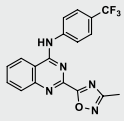	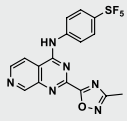	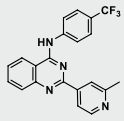	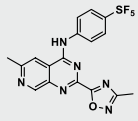	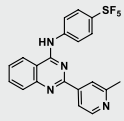
MW	346.179	400.151	371.099	430.064	380.15	444.079	438.094
In vitro HCI cell-based assay: Anti-*Wolbachia* *w*Mel in *D. melanogaster* LDW1 cells							
Anti-*Wolbachia* *w*Mel IC_{50} (nM)	293	89	7	6	21	24	33
Anti-*Wolbachia* *w*Mel IC_{90} (nM)	735	200	43	52	182	1640	283
Ex vivo worm-based assay: Anti-*Wolbachia* *w*Bp in *Brugia pahangi* ovaries							
Anti-*Wolbachia* *w*Bp EC_{50} (nM)	242	97	26	66	51	356	<111
Anti-*Wolbachia* *w*Bp EC_{90} (nM)	799	221	189	346	396	777	<111
% *Wolbachia* *w*Bp elimination at 1 mM	86.3%	98.0%	93.5%	95.5%	94.5%	88.0%	95.5%
In vitro mammalian cytotoxicity assay and compound selectivity							
HEK293T CC_{50} (μM)	10.4	18.6	34.95	15.7	26.8	12.6	2.2
HepG2 CC_{50} (μM)	21.2	30.0	>40	11.3	13.7	9.7	1.6
HEK293T CC_{50}/IC_{50}	35	209	5081	2735	1299	525	66
HepG2 CC_{50}/IC_{50}	72	336	>5816	1968	663	294	49
In vitro *L. loa* microfilaria selectivity							
L. loa microfilaria motility IC_{50} (μM) (ivermectin control IC_{50} = 11.3 μM)	*n/d*	*n/d*	*n/d*	*n/d*	>100	86.9	63.6

of 441 ± 64 nM (Fig. 4, B to D). A similar result was observed with *w*Bm strain of *Wolbachia* in *B. malayi* nematodes, where a 1 μM doxycycline treatment eliminated 72.5% of *Wolbachia* (fig. S3). Benchmarking on this doxycycline activity, we established a validation threshold for our candidate antiwolbachial compounds of ≥75% *w*Bp elimination from the distal ovary at a compound concentration of 1 μM (Fig. 4B).

The ex vivo validation assay could be performed in 11 days, considerably reducing optimization cycle times versus the 3-month-long in vivo validation assays but was labor intensive, relying on nematode dissection and confocal imaging. Thus, on the basis of activity and structural similarity clustering, we chose to test 137 of our 299 primary hits (i.e., the most potent of any closely related analogs; Fig. 4E). Of these, 32 showed a ≥75% *w*Bp elimination at 1 μM, for a validation rate of 23.4% (tables S1 and S5). The percent elimination of *w*Bp in worm ovaries was not generally correlated to compound potency observed in the primary *D. melanogaster* cell-based assay (R^2 = 0.00048; Fig. 4F). Motility of worms was not affected by most of the compounds assayed, with the exception of methylene blue (table S2). Structure analysis of novel molecules demonstrated an enrichment of a quinazoline scaffold among validated compounds: Of 11 quinazolines tested in the secondary assay, 8 quinazolines showed activity superior to doxycycline (Fig. 4F). Members of this series displayed in vitro activity that correlated more with their activity in the ex vivo validation assay (R^2 = 0.3658) compared to all validated compounds (R^2 = 0.0023; Fig. 4G). Because quinazoline heterocycles are present in many of biologically active compounds including antibacterials (*32*, *33*), we focused on this series to improve their physiochemical properties and metabolic stability and their activity against filarial *Wolbachia*.

Quinazoline series demonstrates potent antifilarial *Wolbachia* activity ex vivo and drug-like properties

We carried out a medicinal chemistry campaign to optimize the potency, safety, and physiochemical and pharmacokinetic properties of the quinazoline series, starting with the screen hit CBR008. This involved iterative profiling of analogs in the in vitro cell-based and ex vivo worm-based assays to determine their antiwolbachial activity. Compounds with ≥90% *w*Bp elimination at 1 μM in the worm-based assay underwent absorption, distribution, metabolism, and excretion (ADME) profiling to assess cytochrome P450 (CYP) and human ether-a-go-go related gene (hERG) inhibition (to understand potential drug-drug interaction and cardiotoxicity liabilities of the compounds, respectively), metabolism in human and mouse liver microsomes, permeability in Caco-2 cells, kinetic solubility, and plasma

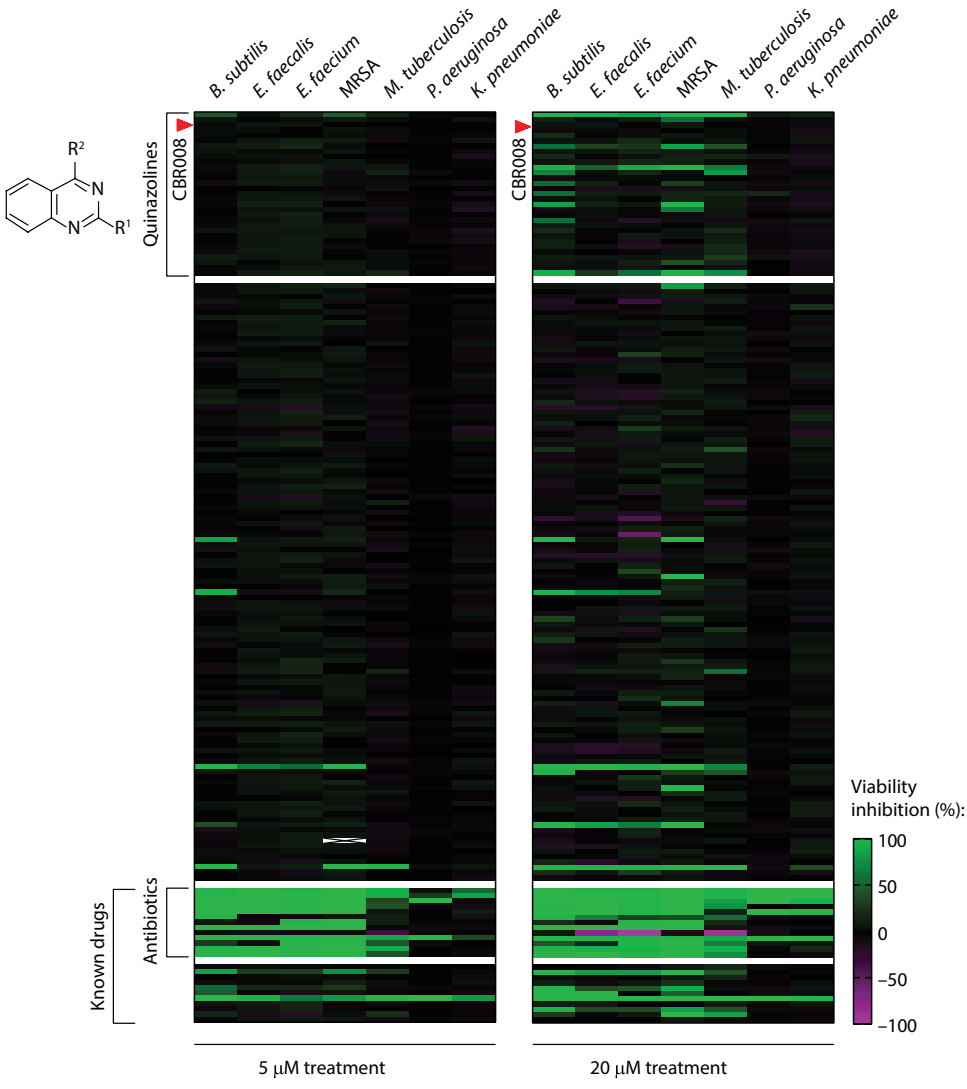

Fig. 2. Novel small molecules with antiwolbachial activity have a narrow antibacterial spectrum. Select powder stocks of compounds identified from Bioactive, Diversity I, and Diversity II libraries that displayed potent and selective antiwolbachial activity were tested against a panel of Gram-positive and Gram-negative bacteria. Bacterial viability inhibition after treatment with 5 or 20 μM of each compound was determined by optical density measurements. MRSA, methicillin-resistant *Staphylococcus aureus*.

protein binding. Analogs with favorable properties (CBR422, CBR625, CBR715, CBR417, and CBR490) were advanced for pharmacokinetic studies in mice (Fig. 5) to determine whether their profiles were suitable for once-a-day (QD) or twice-a-day (BID) dosing in the in vivo preclinical models of infection (e.g., when dosed orally in mice at ≤50 mg/kg maintained plasma exposure over their *w*Bp EC_{90} values for at least 8 hours). As for doxycycline, the quinazoline series compounds had comparable antiwolbachial activity in *B. pahangi* and *B. malayi* worms in the ex vivo assay (determined for CBR422 and CBR625; fig. S3).

Briefly, we found that replacing the amide with an oxadiazole isostere or methylpyridine at the C2 position of the quinazoline core and the trifluoromethyl with a pentafluorosulfanyl group improved the in vitro and ex vivo potencies while increasing metabolic stability and pharmacokinetic properties of the compounds. This effort led to the initial lead CBR422 and the advanced (CBR625 and CBR715) and optimized (CBR417 and CBR490) quinazolines that had excellent potency, selectivity, and ADME properties (Table 1 and table S6). Specifically, compared to screen hit CBR008, these analogs demonstrated improved in vitro and ex vivo potencies (*w*Mel $IC_{50} \leq 33$ nM; *w*Bp $EC_{50} \leq 356$ nM) and an acceptable selectivity index, were orally bioavailable in mice, and had excellent pharmacokinetic properties with a prolonged blood plasma exposure time over EC_{90} when dosed at ≤50 mg/kg (>12 to >24 hours; Fig. 5; table S7). The identified CYP and hERG liabilities of the series (CYP1A2 inhibition IC_{50} of 0.33 μM for initial lead CBR422 and hERG inhibition IC_{50} of 5 μM for CBR625) were markedly reduced in CBR417 (CYP inhibition IC_{50} of ≥30 μM for all isoforms and hERG inhibition IC_{50} of 19.5 μM) and partially addressed in CBR490 (CYP1A2 inhibition IC_{50} of 6.4 μM and hERG inhibition IC_{50} of 7 μM), whereas low kinetic solubility and high protein binding continued to be a feature of the analogs. The advanced and optimized quinazolines were selective against *L. loa* microfilariae (that do not contain *Wolbachia*) in an in vitro motility assay, with IC_{50} values of >100 μM for CBR715, 87 μM for CBR417, and 64 μM for CBR490 versus the 11.3 μM IC_{50} of ivermectin (Table 1).

Optimized quinazoline series demonstrates in vivo efficacy with shortened duration of treatment in preclinical model of filarial infection

A gold-standard in vivo preclinical model for assessing activity of antifilarial compounds within a reasonable period of time uses mice infected with a filarial parasite of rodents, *L. sigmodontis* (Fig. 6A) (*16*, *34*). Because *L. sigmodontis* are hosts to the *Wolbachia* endosymbiont, this is also an excellent preclinical model to assess antiwolbachial compound action, which is performed using qPCR to determine the *Wolbachia ftsZ* gene to the *L. sigmodontis* actin gene ratio in female adult worms recovered from mice at the end of the experiment (4 to 6 weeks after treatment start and 65 to 77 days after infection). A series of studies in this model demonstrated that quinazoline potency in the ex vivo worm-based assay, together with the ability of the compounds to achieve good exposure after oral dosing, were essential for achieving efficacy. For example, an early analog, CBR063, with good ex vivo potency (IC_{50} = 89 nM; EC_{50} = 97 nM) failed to achieve *Wolbachia* clearance in vivo (Fig. 6B), likely due to a comparably inferior pharmacokinetic profile (C_{max} = 119 ± 38.3 ng/ml; Fig. 5A; table S7). However, quinazoline analogs CBR422, CBR625, CBR715, CBR417, and CBR490, with excellent ex vivo

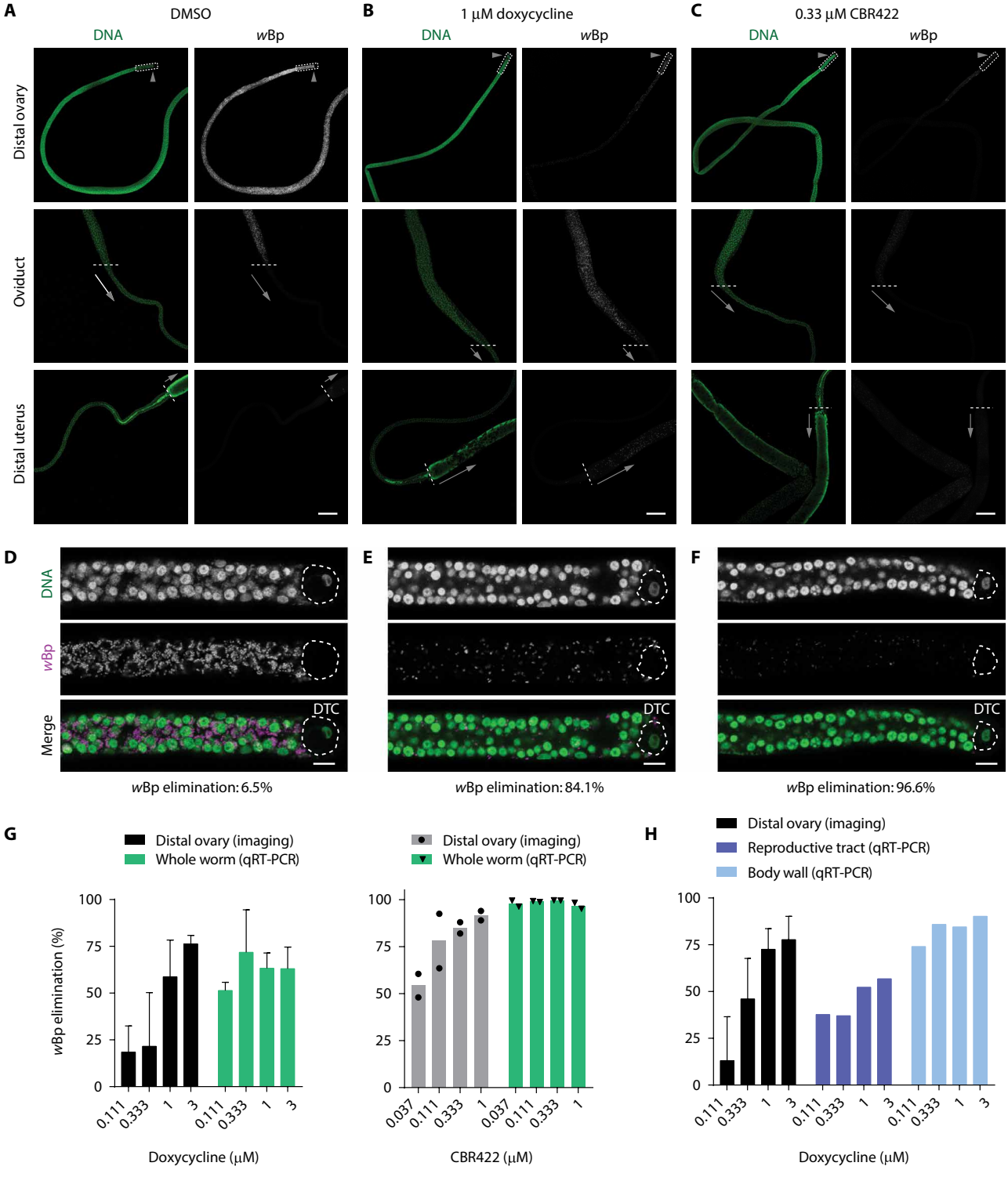

Fig. 3. *Wolbachia* populations in *B. pahangi* adult female worms demonstrate differential susceptibility to antiwolbachial treatment. The effects of short antiwolbachial ex vivo treatments on *Wolbachia* populations within adult female *B. pahangi* worms were evaluated. Worms were treated ex vivo for 3 days with doxycycline or antiwolbachial series lead CBR422, and *Wolbachia* load was quantified using *Wolbachia*-specific 16*S* rRNA FISH and imaging (in distal ovaries) or quantitative reverse transcription polymerase chain reaction (qRT-PCR; in whole worms or tissues). DAPI (green) and *Wolbachia*-specific 16*S* rRNA FISH (white or magenta) staining in ovaries of (**A** and **D**) DMSO-, (**B** and **E**) 1 μM doxycycline–, and (**C** and **F**) 0.33 μM CBR422–treated worms. (A to C) Images of dissected and stained ovaries acquired using a 10× objective of a confocal microscope. Distal ovaries are indicated with boxes and arrowheads; oviducts and distal uteri are indicated with dashed lines and arrows. Scale bars, 100 μm. (D to F) Images of distal ovaries shown in (A) to (C), acquired using a 63× objective of a confocal microscope. Scale bars, 10 μm. *Wolbachia* elimination (%) determined using high-content image analysis is indicated for each section. (**G**) *Wolbachia* quantities in distal ovaries compared to those in whole worms after doxycycline ($n = 3$) or CBR422 ($n = 2$) treatment. (**H**) *Wolbachia* quantities in distal ovaries compared to those in the entire reproductive tract or body wall tissues after doxycycline treatment ($n = 1$). Values for each experiment were normalized to DMSO-treated controls, and means ± SD are shown.

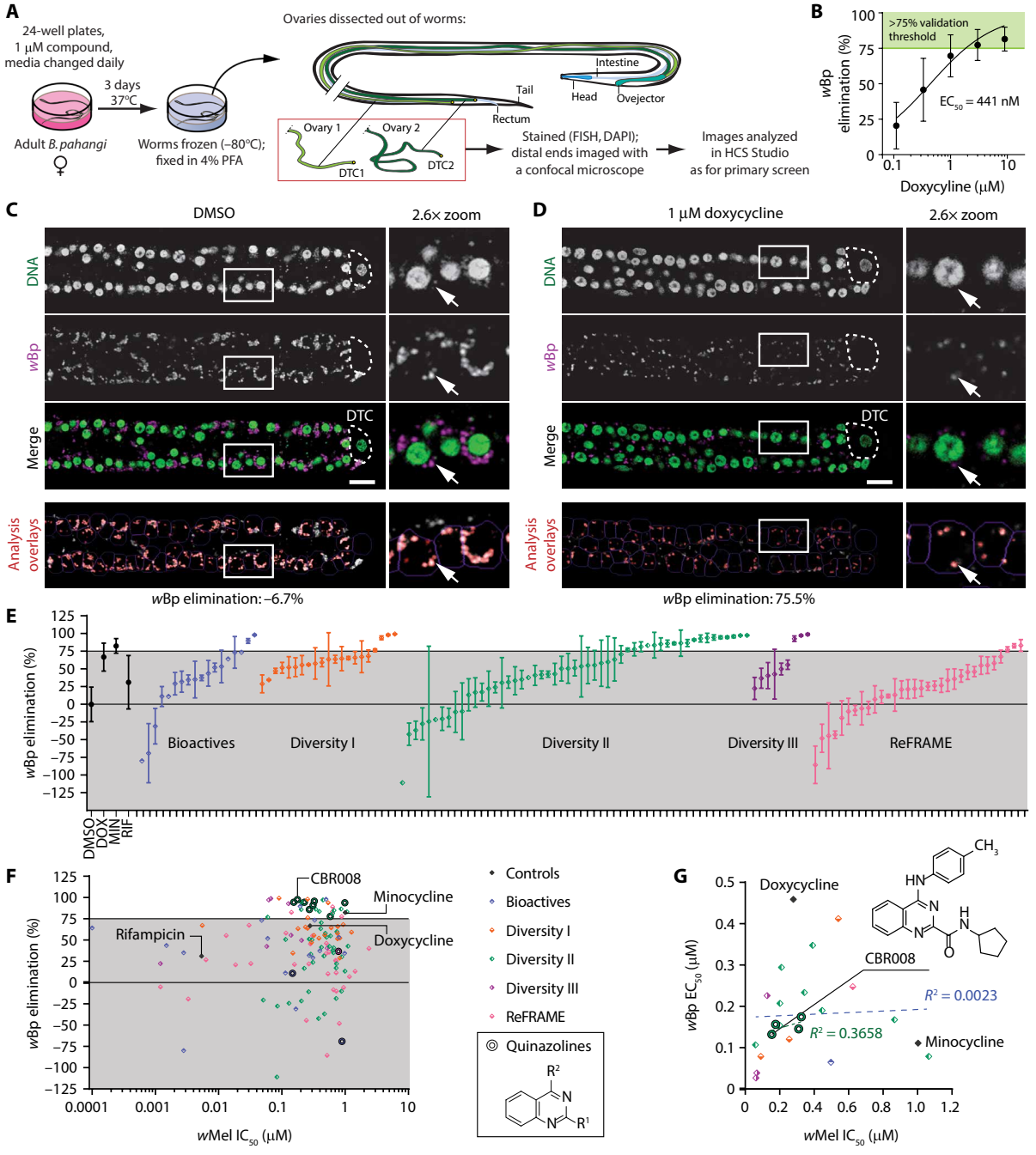

Fig. 4. An ex vivo worm-based validation assay rapidly identifies compounds with antifilarial *Wolbachia* activity. (**A**) Schematic of secondary ex vivo validation screen workflow to assess *Wolbachia* elimination in *B. pahangi* adult worm ovaries. Two worms (yielding a maximum of four ovaries) were included in each treatment. (**B**) Characterization of doxycycline activity against *Wolbachia* within *B. pahangi* ovaries treated ex vivo. The shaded green region indicates the selected validation threshold of >75% *Wolbachia* elimination after 1 μM treatment. Data from >3 separate experiments are plotted as means ± SD. (**C**) Representative images from DMSO- and (**D**) 1 μM doxycycline–treated ovaries stained with DAPI (green) and *Wolbachia* (magenta). Analysis overlays used to quantify *Wolbachia*-specific signal are represented as a semi-transparent red mask. The DTC is indicated with a dashed outline. Scale bars, 10 μm. Boxes surround areas that are magnified 2.6× to the right of each image; arrows indicate *Wolbachia*-specific signal. (**E**) Validation results for potent and selective primary screen hits, tested in the assay at 1 μM. Results are grouped and colored by the library from which each hit originated. Control compounds tested at 1 μM. DOX, doxycycline; MIN, minocycline; RIF, rifampicin. Data are represented as means ± SD (one to four ovaries per treatment). Gray area in the graph represents activities below the set validation threshold. (**F**) *w*Bp elimination in *B. pahangi* worm ovaries plotted against *w*Mel IC_{50} values obtained in the primary insect cell-based assay. Doxycycline, minocycline, and rifampicin controls are indicated, and test compounds are colored by the library from which they originated. Data for quinazolines are indicated as donuts. Gray area in the graph represents activities below secondary assay's validation threshold. (**G**) *w*Bp EC_{50} values obtained for select compounds validated in the secondary worm assay plotted against *w*Mel IC_{50} values obtained in the primary insect cell-based assay. Compounds are labeled according to library origin. Quinazolines are indicated as donuts, and the structure of the most potent, CBR008, is shown. The coefficient of determination (R^2) calculated for all compounds is shown in blue (with the associated regression line; dashed blue) and in green for just the quinazolines.

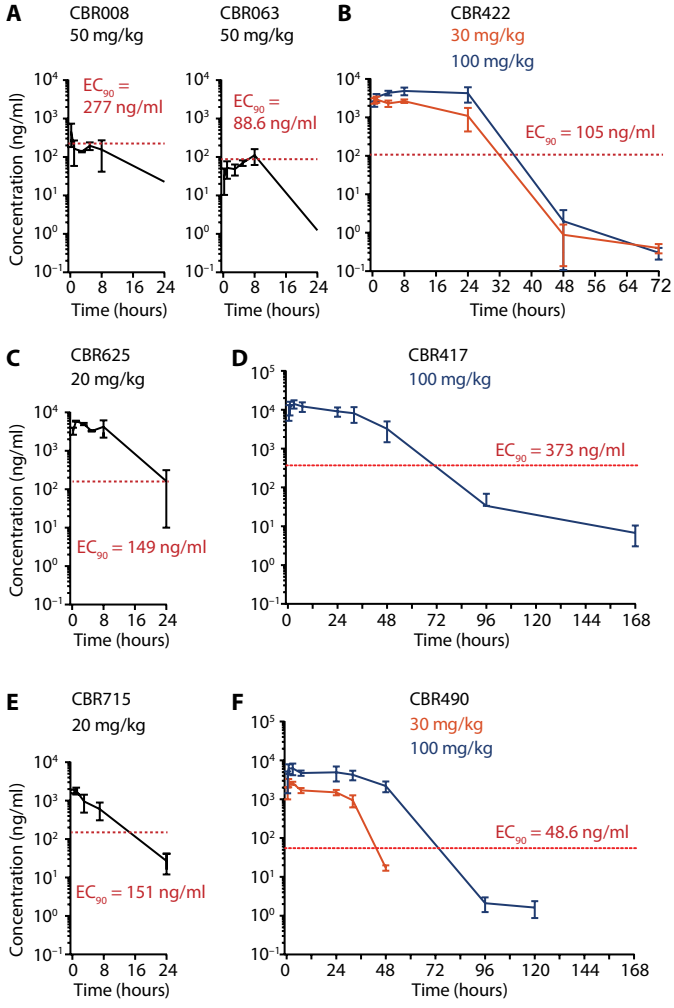

Fig. 5. Optimized quinazoline antiwolbachials demonstrate superior pharmacokinetic profiles. Mice were dosed orally with compounds at indicated amounts. Concentration of each compound in plasma was monitored for at least 24 hours. For each compound, *wBp* EC_{90} values established in the worm-based ex vivo assay are indicated by a red dashed line. Exposure profiles of (**A**) the primary screen hit amide CBR008 and its more potent analog CBR063, (**B**) the oxadiazole series lead CBR422, (**C**) the advanced lead oxadiazole CBR625, (**D**) the optimized series lead oxadiazole CBR417, (**E**) the advanced lead methylpyridine CBR715, and (**F**) the optimized series lead methylpyridine CBR490. CBR008 and CBR063 were formulated in polyethylene glycol 300/5% dextrose in water (3:1, v/v); all other compounds were formulated in 40% (2-hydroxypropyl)-β-cyclodextrin. Means ± SD ($n = 3$ mice) are shown.

potency and pharmacokinetic profiles, all proved efficacious in vivo with <14-day dosing regimens (≤60 mg/kg BID; >99% median *Wolbachia* clearance) and were significantly ($P < 0.05$ to $P < 0.0001$) superior to the 14-day doxycycline control (40 mg/kg BID) ran in parallel (Fig. 6B, fig. S5, and Table 2).

Ability to achieve efficacy in preclinical models with a shortened duration of treatment (≤7 days) is a desired profile because a reduced dosing schedule for an antiwolbachial medication has the potential to facilitate treatment and improve compliance. Therefore, we explored shortened treatment regimens for the efficacious quinazoline analogs. Efficacy (99.80% *Wolbachia* elimination) was achieved with CBR625 7-day dosing (60 mg/kg BID) and near-target efficacy (98.95% elimination) with dosing (60 mg/kg QD; fig. S5A and Table 2). Likewise, an oral 7- and 12-day treatment of CBR715 at 50 mg/kg BID eliminated 98.86 and 99.80% of *Wolbachia*, respectively (Fig. 6B and Table 2). Sparse pharmacokinetics (PK) sampling during in vivo studies confirmed relative exposures of the tested quinazolines (fig. S4). Furthermore, an oral 4-day treatment at 60 mg/kg QD with the optimized quinazolines eliminated 99.80% (CBR490) and 99.96% (CBR417) of *Wolbachia* in *L. sigmodontis* adult female worms, significantly superior ($P = 0.0013$ for CBR490 and $P < 0.0001$ for CBR417) to the 14-day doxycycline control ran in parallel (95.21% elimination; Fig. 6B and Table 2).

Because of the demonstrated potency and favorable exposures of optimized quinazolines CBR417 and CBR490 [time over EC_{90} of 72 hours for a single oral dose (100 mg/kg); table S7], we investigated whether an even more markedly abbreviated efficacious dosing regimen with these compounds was attainable. Both CBR417 and CBR490 were dosed at 100 mg/kg once per week over a 2-week period (two doses total) in the mouse/*L. sigmodontis* model, and a single dose (200 mg/kg) was also evaluated. All treatment regimens eliminated >99% of *Wolbachia* in *L. sigmodontis* adult female worms, significantly superior ($P < 0.01$) to the 14-day doxycycline control ran in parallel (95.21% elimination; Fig. 6B and Table 2). Examination of in vivo efficacy in response to diverse dosing regimens showed that the dose of CBR490 was equally correlated to in vivo efficacy ($R^2 = 0.7263$) as was total dose ($R^2 = 0.713$; fig. S6). Too few data points were available for CBR417 to make a conclusive analysis.

CBR417 and CBR490 demonstrate favorable safety profiles in preclinical studies

CBR417 and CBR490 safety profiles were more extensively assessed (Table 3). Both compounds were well tolerated in mouse in vivo efficacy studies, even when administered at high doses (200 mg/kg; single dose) or for prolonged periods of time [CBR490 daily total dose (60 mg/kg) for 11 days]. Neither compound showed intrinsic mutagenic potential based on negative results in mini-Ames, in either the absence or the presence of rat liver S9 mix for metabolic activation. Micronucleus assays also did not reveal inherent genotoxicity potential. The CBR417 oxadiazole did not strongly inhibit hERG or CYP enzymes (the latter assessed for potential drug-drug interactions), and neither compound caused human pregnane X receptor (PXR) activation (a hallmark of CYP3A4 induction). A prospective cardiovascular liability due to hERG inhibition was identified for CBR490 in preliminary profiling assays ($IC_{50} = 7.07$ μM); however, a cardiac safety panel revealed no significant hits for either compound (table S8). To explore other potential off-target effects that could lead to in vivo toxicity, the Eurofins Cerep-Panlabs safety screen against 44 selected targets was carried out and identified 12 targets significantly inhibited (>50%) by CBR490 and only three inhibited by CBR417 (table S9). In summary, these findings demonstrate the favorable safety profiles of CBR417 and CBR490 quinazolines.

Advanced quinazoline lead eliminates *Wolbachia* in *B. malayi* and *Onchocerca* adult worms in vivo

Because of the demonstrated efficacy of optimized quinazoline analogs against *Wolbachia* in *L. sigmodontis*, we assayed one of these advanced leads (CBR715) for efficacy in preclinical murine models of *B. malayi* and *Onchocerca* adult worm infections. Retention of compound activity in the *Onchocerca* model was of particular concern because both the *Wolbachia* endosymbionts and the *Onchocerca* hosts are more distantly related from the above host/endosymbiont models:

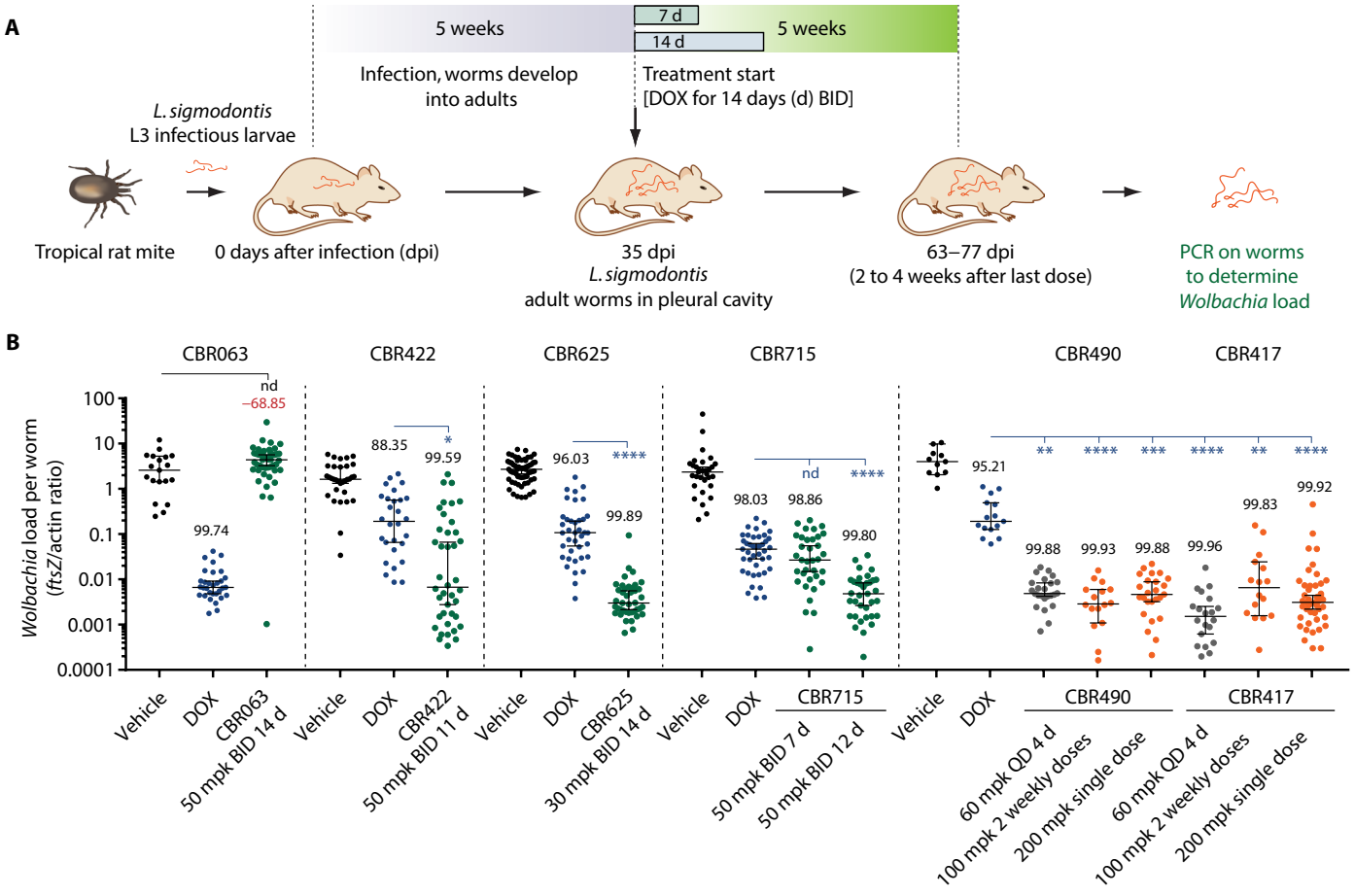

Fig. 6. Quinazolines demonstrate antiwolbachial efficacy in mouse model of *L. sigmodontis* filarial infection. (**A** and **B**) Advanced antiwolbachial compounds were assayed in an in vivo model of *L. sigmodontis* filarial infection where mice ($n = 4$ to 6 per group) infected with adult *L. sigmodontis* filarial worms (infected by mites carrying *L. sigmodontis* infectious larvae) are dosed for up to 14 days with a compound of interest. (B) *Wolbachia* load per worm was determined by the ratio of *Wolbachia ftsZ* gene to that of filarial actin. Vehicle control and a 14-day doxycycline control (40 mg/kg BID) were included in each independent experiment. Medians with 95% confidence interval are shown, and median elimination (%) is reported. mpk, mg/kg; nd, no significant difference. *$P < 0.05$, **$P < 0.01$, ***$P < 0.001$, ****$P < 0.0001$.

Wolbachia of *Onchocerca* species belong to supergroup C, whereas *Wolbachia* of the more closely related *L. sigmodontis* and *Brugia* spp. belong to supergroup D (*35*–*37*). The only available in vivo model of *Onchocerca* adult worms uses the bovine parasite *O. ochengi* (*38*), which is a sister species and the closest relative of the human river blindness parasite, *O. volvulus* (*39*).

The severe combined immunodeficient (SCID) mouse *B. malayi* and *O. ochengi* models were previously described and, similar to the mouse/*L. sigmodontis* efficacy model, rely on qPCR for quantification of filarial *Wolbachia* (*38*). In the *B. malayi* in vivo model (Fig. 7A), treatments with CBR715 (7- and 14-day dosing schedules at 50 mg/kg BID) eliminated >99% *Wolbachia* in *B. malayi* adult females, with the 14-day CBR715 treatment eliminating significantly more *Wolbachia* ($P = 0.0464$) compared to the 42-day doxycycline control (Fig. 7B). Doxycycline (42 days) and both CBR715 treatments eliminated all circulating microfilariae (Fig. 7C), and although a general trend of reduced adult worm burden was observed, these differences were not statistically significant ($P > 0.05$; Fig. 7D). Likewise, in the *O. ochengi* in vivo model (Fig. 7E), 7- and 14-day treatments with CBR715 eliminated >99% *Wolbachia* in *O. ochengi* adult males, on par with the 28-day doxycycline treatment control (Fig. 7F), and no difference in percent recovery of implanted males was observed (Fig. 7G). These data confirm the broad spectrum of activity of the optimized antiwolbachial quinazoline series and the continued superior performance of this series compared to doxycycline in in vivo preclinical rodent models of diverse filarial infections.

DISCUSSION

Here, we describe an accelerated drug discovery platform for the identification of antiwolbachial compounds and translation of these to efficacious leads in in vivo models of filarial infection. Previous screening efforts using high-throughput insect cell-based assays have identified antiwolbachial compounds active in vitro, yet translation of these hits to in vivo models and the clinic has been challenging for a number of reasons. First, *Wolbachia* are obligate intracellular bacteria and may only be propagated within appropriate host cells. Because no nematode cell lines have been developed, for high-throughput screening drug discovery, researchers have relied on insect cell lines infected with *Wolbachia* strains that are specific to these hosts (*25*, *28*, *40*–*42*). Fortuitously, there are substantial similarities in the genetics and cell biology of the *Wolbachia* species

Table 2. *Wolbachia* elimination from female adult worms achieved after quinazoline treatment in the mouse/*L. sigmodontis* in vivo model of filarial infection. For ease of interpretation, efficacy values are presented in table cells colored on a sliding scale with excellent efficacy (>99 to 98% elimination of *Wolbachia*) in green, medium levels of efficacy (95 to 80% elimination) in yellow, and inferior levels in orange (70 to 40% elimination) and red (<30% elimination).

Dose (mpk)		Days of dosing														CBR063	CBR422	CBR625	CBR715		CBR417	CBR490
		1	2	3	4	5	6	7*	8	9	10	11	12	13	14							
BID dosing	100	••	••	••	••	••	••													99.88%		
	60	••	••	••	••	••	••	••											99.80%			
	60	••	••	••	••	••	•															99.91%
	50	••	••	••	••	••	••	••	••	••	••	••	••	••	••		−68.85%					
	50	••	••	••	••	••	••	••	••	••	••	••	••							99.80%		
	50	••	••	••	••	••	••	••	••	••	••	••						99.59%				
	50	••	••	••	••	••	••	••												98.86%		
	30	••	••	••	••	••	••	••	••	••	••	••	••	••	••				99.89%			
	30	••	••	••	••	••	••	••	••	••	••	••										99.68%
	30	••	••	••	••	••	••	••	••	•									98.86%			
	30	••	••	••	••	••	••	••											93.20%	57.75%		
	10	••	••	••	••	••	••	••											66.43%			
QD dosing	60	•	•	•	•	•	•	•											98.95%	48.59%		99.72%
	60	•	•	•	•	•	•														99.61%	
	60	•	•	•	•																99.96%	99.88%
	30	•	•	•	•	•	•	•											42.86%			99.94%
	30	•	•	•	•																	80.73%
	10	•	•	•	•	•	•	•											54.29%			55.14%
Weekly	200	•																			99.92%	99.88%
	100	•							•												99.83%	99.87%†

*Desired dosing profile for a macrofilaricide: Oral dose, once daily, up to 7 days or single, intramuscular injection. †Mean of two independent experiments.

that warrant using the infected insect cell lines as a primary screen and a high-throughput proxy for filarial *Wolbachia*-based assays. However, there are also considerable differences between *Wolbachia* strains, demonstrated not only by host range but also by their genomes. For example, Foster *et al.* (*43*) reported a greater reduction of *B. malayi Wolbachia w*Bm genome (in total size and predicted gene number) compared to *D. melanogaster Wolbachia w*Mel. Thus, compounds identified in whole-cell screens against insect *Wolbachia* may hit targets that are sufficiently divergent or even absent in filarial *Wolbachia*. Similarly, compounds that target a host cell factor to reduce *Wolbachia* load may be absent in filarial nematodes. Last, filarial nematodes may shelter *Wolbachia* from compound action through limited permeability, compound metabolism, and/or excretion.

To address these limitations, following up on initial studies (*25*), we developed an orthogonal assay in filarial nematodes that allowed us to rapidly assess antifilarial *Wolbachia* activity of our primary screen hits. We used *B. pahangi*, a filarial parasite of cats that can also infect humans (*44*), because these worms are closely related to *B. malayi* (*45*) but can be maintained in an animal host (jirds) in larger quantities and, therefore, are more readily available. We focused our evaluation of *Wolbachia* load within worm ovaries for a number of reasons because this population appeared less sensitive to compound treatment than *Wolbachia* in the hypodermal chords of the animals, providing a more rigorous and pertinent readout of antiwolbachial compound action. A similar differential susceptibility to compound action in the hypodermis versus the ovaries has been previously observed in vivo in *O. ochengi* adult worms after antibiotic treatments in cattle (*31*). The difficulty in eliminating different clades of *Wolbachia* from ovaries of different species of worms (*Wolbachia* supergroup D in *Brugia* spp. reported here and supergroup C in *Onchocerca* spp.) further supports the relevance of this tissue for assessment of antiwolbachial compound efficacy. We used *Wolbachia* 16*S* rRNA FISH to detect the bacteria in both the cell-based high-throughput assay and the ex vivo worm-based assay. In addition to its inherent specificity, rRNA provides a more sensitive viability metric because it is less stable than DNA, allowing us to observe *Wolbachia* elimination in worm ovaries after only a relatively short 3-day treatment ex vivo. Although true markers of viability can be challenging to use in high-throughput screens, this approach gave us confidence in our ability to select fast-acting, antifilarial *Wolbachia* compounds.

In our primary insect cell-based screen, we identified known drugs with potent and selective antiwolbachial activity. Among these were antineoplastics and signal transduction modulators, which potentially exert their activity by affecting host cell processes exploited or required by this obligate intracellular bacterium. For example, *Wolbachia* has been found to alter lipid metabolism of mosquitoes

Table 3. In vitro ADME and safety profiling data for optimized leads CBR417 and CBR490. $T_{1/2}$, half-life; M/R/D/H, mouse/rat/dog/human; CLint, intrinsic clearance; MDCK-MDR1, Madin-Darby canine kidney cells transfected with the human *MDR1* gene; Papp, apparent permeability coefficient.

	CBR417	CBR490
	Oxadiazole	Methylpyridine
Molecular weight (Da)	444.079	438.094
Solubility (pH 6.8) (μM)	1	1
Melting point (°C)	149–153	250–253
Lipohilicity (cLogP)	4.44	6.18
Plasma protein binding	>99.9% (human)	98.08% (human)
	>99.9% (mouse)	>99.9% (mouse)
Permeability Caco-2		
Papp A-B (10^{-6} cm/s)	2.08	0.14
Papp B-A (10^{-6} cm/s)	1.79	0.26
Metabolic stability (M/R/D/H)		
Extraction ratio (%)	52/20/30/41	86/35/39/63
$T_{1/2}$ (min)	56/145/145/88	10/85/100/35
CL_{int} (μL/min per mg)	25/10/10/16	137/16/14/39
hERG (cardiotoxicity)—manual patch clamp		
% Inhibition at 5 μM	20.5	27.1
IC_{50} (μM)	19.5	7.1
Cardiac panel safety profiling*	No significant inhibition	No significant inhibition
Mini-Ames (genotoxicity)	Negative	Negative
Micronucleus induction (mutagenicity)	Negative	Negative
CYP isoform (IC_{50}) (μM)		
Reversible 1A2	29.52	6.38
Reversible 2C19	>50	11.25
Reversible 2C9	45.34	6.81
Reversible 2D6	>50	13.00
Time-dependent inhibition 3A4	>50	>50
CYP induction, PXR functional assay	>30	>30
Safety pharmacology profiling† (selected receptors, ion channels, transporters, kinases, etc.)	4 with >45% binding/ inhibition	14 with >45% binding/inhibition
P-glycoprotein inhibition, MDCK-MDR1 IC_{50} (μM)	6.5	1.49

*Table S8. †Table S9.

(*46*), and insulin signaling and the target of rapamycin (TOR) complex 1 pathway have been implicated in controlling *Wolbachia* titers in *D. melanogaster* (*47*, *48*). Accordingly, in our screen, we identified mammalian target of rapamycin (mTOR) inhibitors and drugs affecting cellular metabolism (e.g., drugs for diabetes and liver X receptor agonists). We also identified many antibiotics with antiwolbachial activity, including ones belonging to antibiotic classes that have been previously identified in similar insect cell-based screens and assays [tetracyclines, rifamycins, pleuromutilins, fluoroquinolones, and macrolides (ABBV-4083, an orally available derivative of the macrolide antibiotic tylosin, is currently being developed as an antiwolbachial therapy)] (*27*, *28*, *41*, *49*, *50*) and others that, to our knowledge, have not been previously reported (aminocoumarins and peptide deformylase inhibitors). We found that most of these known drugs and antibiotics did not efficiently eliminate *Wolbachia* from *B. pahangi* ovaries in our ex vivo validation assay, regardless of their impressive potency in vitro. Therefore, although we relied on the high-throughput assay to identify potential antiwolbachials, developing and using an orthogonal assay that evaluated compound efficacy against *Wolbachia* in parasitic worms allowed us to prioritize molecules with rapid antifilarial *Wolbachia* activity for further medicinal chemistry optimization.

The desired profile for an antiwolbachial macrofilaricide compound is the ability to cause >99% depletion of *Wolbachia* in adult worms within 7 days of dosing in all three preclinical models of filarial disease (*L. sigmodontis*, *B. malayi*, and *O. ochengi*). The oxadiazole and methylpyridine leads (CBR625, CBR417, CBR715, and CBR490) proved efficacious in vivo, causing a >99% *Wolbachia* elimination in adult *L. sigmodontis* worms within the mandated dosing schedule of ≤7 days. In addition, the advanced methylpyridine lead CBR715 recapitulated this in vivo efficacy against *Wolbachia* in human parasite *B. malayi* and a close surrogate of *O. volvulus* (*O. ochengi*), demonstrating real promise in translation of the quinazoline series to a cure for human filarial infections. Our optimization strategy ultimately led to synthesis of leads CBR490 and CBR417 that, with just a single dose, were efficacious in vivo at eliminating >99% of *Wolbachia* from adult *L. sigmodontis* female worms. Abbreviated dosing schedules have a real advantage in treating infections in resource-limited countries and elsewhere because compliance and point of care distribution are greatly facilitated. Last, both CBR417 and CBR490 demonstrated safety in initial in vivo and in vitro preclinical profiling and did not show strong activity in vitro against *L. loa* microfilariae (IC_{50} = 87 and 64 μM, respectively) compared to the ivermectin control (IC_{50} = 11.3 μM), suggesting that they would be appropriate for administration to patients in *L. loa*–endemic regions after further safety assessments against *L. loa* microfilariae in vivo.

Despite the promise of these results, we note limitations and outstanding questions that need to be addressed before clinical translation of this work. Because of the length of time (years) needed for adult worm death after *Wolbachia* elimination, reduction in worm numbers in the murine assays is not anticipated and was not observed. However, the more immediate phenotype of worm sterilization was observed in the *B. malayi* murine model. Currently, we also have no evidence that the observed *Wolbachia* elimination is sustained beyond 4 to 5 weeks after treatment, and studies using in vivo jird models that can accommodate patent filarial infections for at least 6 months (*51*) are necessary to determine the lowest efficacious dose of quinazolines that prevent *Wolbachia* recrudescence. Last, treatment of the large, long-lived female worms belonging to the *Onchocerca* spp. represents the ultimate challenge, with females containing 20× more *Wolbachia* than males (*52*). Therefore, further assessment of quinazoline efficacy in models that support *Onchocerca* female worms in vivo (such as the bovine model of infection) will likewise be required to determine efficacious dosing regimens.

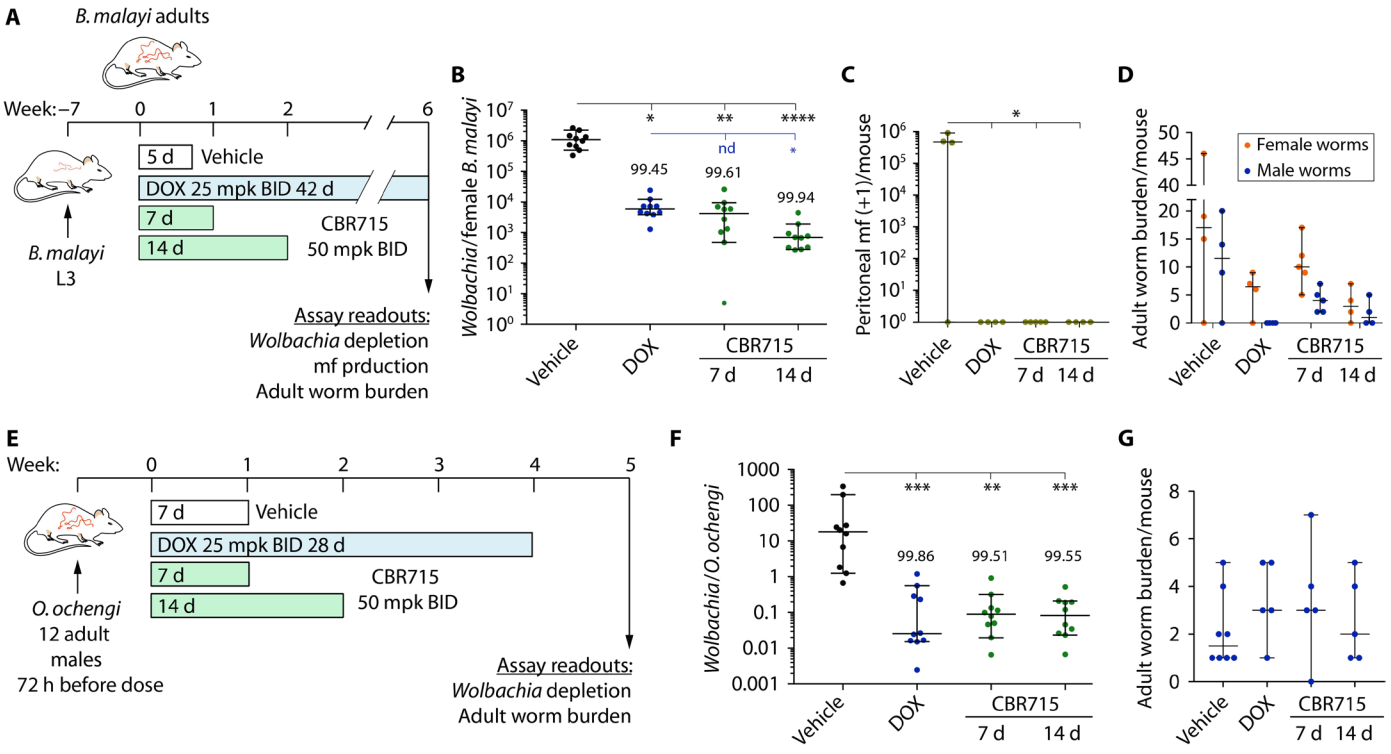

Fig. 7. Quinazoline CBR715 demonstrates antiwolbachial efficacy in mouse models of *B. malayi* and *O. ochengi* filarial infection. (**A**) Efficacy of CBR715 against *Wolbachia* in *B. malayi* was assessed in a mouse model of infection where mice ($n = 6$ per group) are inoculated with infectious L3 larvae of *B. malayi*. (**B**) *Wolbachia* content in adult worms determined 6 weeks after the beginning of treatment is shown. Effect of CBR715 and doxycycline control treatments on (**C**) the number of microfilariae (mf) circulating in the blood and (**D**) total *B. malayi* worm burden at the end of the in vivo experiments is shown. (**E**) Advanced lead CBR715 efficacy against *Wolbachia* in *O. ochengi* was assessed in a mouse model of infection where mice ($n = 6$ per group) are implanted with *O. ochengi* adult male worms. (**F**) *Wolbachia* content in adult worms determined 5 weeks after the beginning of treatment. (**G**) Effect of CBR715 and doxycycline control treatments on total *O. ochengi* male worms recovered at the end of the in vivo experiments. To assess significance between treatment groups, we used the nonparametric Kruskal-Wallis test with Dunn's multiple comparison test. Black lines indicate significant differences between vehicle control and treatment groups, and blue lines indicate significant differences between doxycycline and treatment groups. $^*P < 0.05$, $^{**}P < 0.01$, $^{***}P < 0.001$, $^{****}P < 0.0001$.

Recently, chemical optimization of the thienopyrimidine series identified in high-throughput screening led to the generation of AWZ1066, a compound with a quinazoline scaffold and increased efficacy against both insect and filarial *Wolbachia* (*53*). However, quinazoline heterocycles are present in many biologically active compounds, and whether CBR417, CBR490, and AWZ1066 share the same mechanism of action is uncertain. Genetic manipulation of *Wolbachia* has not been developed, and its obligate intracellular lifestyle complicates target identification efforts, such as evolution of resistance and confirmation of putative targets via genetic means. AWZ1066 and many novel scaffolds identified in our primary screen, including the prototypical quinazoline CBR008, demonstrated very specific antibacterial spectrum of activity, which may indicate a *Wolbachia*- or *Wolbachia* host–specific target. This also suggests that the quinazolines may be narrow spectrum antibiotics, a favorable profile for treating filarial nematode infections while reducing the effects of treatment on the microbiomes of treated individuals.

In summary, our antiwolbachial drug development platform enabled the path toward a short-course oral therapy for elimination of *Wolbachia*-reliant filarial nematodes, including ones that cause lymphatic filariasis and onchocerciasis. Our work supports advancement of the oxadiazole and methylpyridine quinazoline subseries for additional preclinical safety assessment and indicates that quinazolines are a selective treatment for currently intractable filarial worm infections.

MATERIALS AND METHODS

Study design

The objective of this study was to identify antifilarial *Wolbachia* compounds with efficacy superior to that of doxycycline when administered with an abbreviated dosing schedule (≤7 days). *Wolbachia*-infected *Drosophila* cell-based high-content imaging assay was used to screen for potent antiwolbachial compounds, and putative hits were counterscreened in mammalian cells. Activity of potent and selective compounds was validated in an ex vivo whole-worm assay observing filarial *Wolbachia* reduction in *B. pahangi* adult female ovaries, benchmarking on doxycycline activity. In vivo experiments were designed to compare *Wolbachia* reduction in *L. sigmodontis*, *O. ochengi*, or *B. malayi* adult worms between different treatment groups, a gold standard doxycycline and a vehicle control, in a randomized design with multiple arms and shared controls. The *Wolbachia* single gene *ftsZ*/worm actin ratios were compared to the vehicle and doxycycline treatment. Where applicable, sample size, selection, blinding schemes, and replicates are provided in the figure legends, and in the Materials and Methods. Primary data are reported in data file S1.

Primary in vitro cell-based assay

Wolbachia-infected LDW1 cells (*26*) were maintained in Shields and Sang M3 (SSM3) insect medium (Sigma-Aldrich) supplemented with 10% heat-inactivated FBS (qualified, One Shot format, Gibco) at 25°C, in flasks with unvented caps. Assay plates (Greiner, part nos. 789071 and 789091) were prepared by coating with 0.5 mg/ml (384-well plates) or 1 mg/ml (1536-well plates) solution of concanavalin A lectin (MP Biomedicals). Compounds were acoustically transferred into coated plates using the Echo 555 Liquid Handler (Labcyte Inc.). Cells were trypsinized (TrypLE Express, Gibco), scraped, and seeded at 12,000 cells per well (384-well plates) or 4000 cells per well (1536-well plates) in SSM3 medium supplemented with 2% FBS. Plates were spun at 800 rpm for 3 min and incubated at 25°C. Six days after seeding, cells were fixed with 4% PFA for at least 10 min and washed with phosphate buffered saline (pH 7) and 0.1% Tween 20 (PBS-T). FISH was used to stain *Wolbachia*, and 3 μM DAPI was used to stain DNA. The MultiFlo FX Multi-Mode Dispenser (BioTek) was used for concanavalin A coating, cell fixation, and staining of 384-well plates, and the "bottle valve" dispenser with an angled head (Kalypsys Inc.) was used for processing of 1536-well plates. Plates were imaged using the CX5 CellInsight Cellomics high-content imaging instrument with a 10× objective (Thermo Fisher Scientific). Each well was analyzed using compartmental analysis in HCS Studio (Thermo Fisher Scientific) for cell number and *Wolbachia* content (see Supplementary Materials and Methods).

Orthogonal ex vivo *Brugia* validation assay

Adult *B. pahangi* and *B. malayi* females cultivated in and extracted from peritoneal cavities of jirds (*Meriones unguiculatus*) were obtained mainly from TRS Laboratories. *B. pahangi* were also provided by B. T. Beerntsen (University of Missouri) and the National Institutes of Health (NIH)/National Institute of Allergy and Infectious Diseases (NIAID) Filariasis Research Reagent Resource Center for distribution by BEI Resources, NIAID, NIH [adult female *B. pahangi* (live), NR-48903]. After shipment, worms were immediately separated into 24-well plates, one animal per well, and allowed to recover for 2 days in high-glucose RPMI 1640 medium (the American Type Culture Collection modification; Gibco) supplemented with 10% minimum essential medium (Gibco) and 10% heat-inactivated HyClone FBS (GE Healthcare Life Sciences). Media were changed daily, and compounds were tested at indicated concentrations (0.1% DMSO). Gross motility of worms was observed by eye during treatment and compared to DMSO controls. After 3 days of treatment, animals were frozen at −80°C, thawed, and fixed for 20 min with 3.2% PFA in PBS-T. Ovaries were dissected out, stained for *Wolbachia* using a modified FISH protocol, mounted on slides using VECTASHIELD with DAPI mounting medium (H-1200, Vector Laboratories Inc.) and imaged using a confocal microscope (see Supplementary Materials and Methods). To reduce variability, worms originating from a single jird were used in each experiment. The experiments were carried out partially blinded because, with the exception of DMSO and doxycycline controls, the identity of tested compounds was masked during treatment, imaging, and analysis.

Statistical analysis

Percentage *Wolbachia* reduction in macrofilariae was normalized to median vehicle control values derived from the same experimental infection and screen. Where available, repeat experimental data were pooled after normalization. For analysis of *Wolbachia* depletion in in vivo experiments, where the majority of grouped data failed the D'Agostino and Pearson normality test ($P > 0.05$), a nonparametric Kruskal-Wallis test with Dunn's correction for multiple comparisons was used to determine significance, and medians with 95% confidence intervals are shown. Comparisons between vehicle and all treatment groups and doxycycline and all treatment groups were preselected. All statistics were computed using GraphPad Prism v6.0h.

SUPPLEMENTARY MATERIALS

stm.sciencemag.org/cgi/content/full/11/491/eaav3523/DC1

Materials and Methods

Fig. S1. Classes of known drugs and bioactive molecules identified as potent and selective antiwolbachial hits in the primary in vitro screen.

Fig. S2. *Wolbachia* distribution in ovaries and the hypodermis of DMSO-treated worms.

Fig. S3. *Wolbachia* elimination from *B. malayi* worm ovaries ex vivo.

Fig. S4. Sparse pharmacokinetic profiles of quinazoline antiwolbachials during efficacy studies.

Fig. S5. *Wolbachia* elimination after quinazoline treatment in the mouse/*L. sigmodontis* in vivo model of filarial infection.

Fig. S6. CBR417 and CBR490 dose-response relationship based on *Wolbachia* elimination in mouse/*L. sigmodontis* efficacy studies.

Table S1. Primary and validation screen statistics.

Table S2. Antiwolbachial activities of known drugs and bioactive molecules identified as potent and selective hits in the primary in vitro screen (powders and ReFRAME compounds).

Table S3. Antibacterial activities of primary screen hits from Bioactive, Diversity I, and Diversity II libraries.

Table S4. Activity of optimized antiwolbachial leads against a panel of Gram-positive and Gram-negative bacteria.

Table S5. Activities of screening hits validated ex vivo worm-based assay (all except ReFRAME compounds are powders).

Table S6. ADMET properties of quinazoline antiwolbachials.

Table S7. Pharmacokinetic properties of antiwolbachial quinazolines.

Table S8. Cardiac panel study results for CBR417 and CBR490.

Table S9. Safety pharmacology profiling study results for CBR417 and CBR490.

Data file S1. Primary data.

References (*54*–*67*)

REFERENCES AND NOTES

1. Global Burden of Disease Study 2013 Collaborators, Global, regional, and national incidence, prevalence, and years lived with disability for 301 acute and chronic diseases and injuries in 188 countries, 1990-2013: A systematic analysis for the Global Burden of Disease Study 2013. *Lancet* **386**, 743–800 (2015).
2. World Health Organization, *Investing to Overcome the Global Impact of Neglected Tropical Diseases: Third WHO Report on Neglected Diseases 2015* (World Health Organization, 2015).
3. World Health Organization, "Global health estimates 2014 summary tables: YLD by cause, age and sex, 2000–2012" (2014).
4. D. Gems, Longevity and ageing in parasitic and free-living nematodes. *Biogerontology* **1**, 289–307 (2000).
5. J. Lawrence, Y. K. Sodahlon, K. T. Ogoussan, A. D. Hopkins, Growth, challenges, and solutions over 25 years of mectizan and the impact on onchocerciasis control. *PLOS Negl. Trop. Dis.* **9**, e0003507 (2015).
6. M. Y. Osei-Atweneboana, K. Awadzi, S. K. Attah, D. A. Boakye, J. O. Gyapong, R. K. Prichard, Phenotypic evidence of emerging ivermectin resistance in *Onchocerca volvulus*. *PLOS Negl. Trop. Dis.* **5**, e998 (2011).
7. C. N. Pulaski, J. B. Malone, C. Bourguinat, R. Prichard, T. Geary, D. Ward, T. R. Klei, T. Guidry, G. Smith, B. Delcambre, J. Bova, J. Pepping, J. Carmichael, R. Schenker, R. Pariaut, Establishment of macrocyclic lactone resistant *Dirofilaria immitis* isolates in experimentally infected laboratory dogs. *Parasit. Vectors* **7**, 494 (2014).
8. R. M. Kaplan, A. N. Vidyashankar, An inconvenient truth: Global worming and anthelmintic resistance. *Vet. Parasitol.* **186**, 70–78 (2012).
9. R. J. Kastner, C. M. Stone, P. Steinmann, M. Tanner, F. Tediosi, What is needed to eradicate lymphatic filariasis? A model-based assessment on the impact of scaling up mass drug administration programs. *PLOS Negl. Trop. Dis.* **9**, e0004147 (2015).
10. K. K. Frempong, M. Walker, R. A. Cheke, E. J. Tetevi, E. T. Gyan, E. O. Owusu, M. D. Wilson, D. A. Boakye, M. J. Taylor, N. K. Biritwum, M. Osei-Atweneboana, M. G. Basanez, Does increasing treatment frequency address suboptimal responses to ivermectin for the control and elimination of river blindness? *Clin. Infect. Dis.* **62**, 1338–1347 (2016).

11. B. V. Babu, G. R. Babu, Coverage of, and compliance with, mass drug administration under the programme to eliminate lymphatic filariasis in India: A systematic review. *Trans. R. Soc. Trop. Med. Hyg.* **108**, 538–549 (2014).
12. L. Senyonjo, J. Oye, D. Bakajika, B. Biholong, A. Tekle, D. Boakye, E. Schmidt, E. Elhassan, Factors associated with ivermectin non-compliance and its potential role in sustaining *Onchocerca volvulus* transmission in the west region of Cameroon. *PLOS Negl. Trop. Dis.* **10**, e0004905 (2016).
13. D. H. Molyneux, A. Hopkins, M. H. Bradley, L. A. Kelly-Hope, Multidimensional complexities of filariasis control in an era of large-scale mass drug administration programmes: A can of worms. *Parasit. Vectors* **7**, 363 (2014).
14. R. Stouthamer, J. A. Breeuwer, G. D. Hurst, *Wolbachia pipientis*: Microbial manipulator of arthropod reproduction. *Annu. Rev. Microbiol.* **53**, 71–102 (1999).
15. S. C. Bosshardt, J. W. McCall, S. U. Coleman, K. L. Jones, T. A. Petit, T. R. Klei, Prophylactic activity of tetracycline against *Brugia pahangi* infection in jirds (*Meriones unguiculatus*). *J. Parasitol.* **79**, 775–777 (1993).
16. A. Hoerauf, K. Nissen-Pähle, C. Schmetz, K. Henkle-Dührsen, M. L. Blaxter, D. W. Büttner, M. Y. Gallin, K. M. Al-Qaoud, R. Lucius, B. Fleischer, Tetracycline therapy targets intracellular bacteria in the filarial nematode *Litomosoides sigmodontis* and results in filarial infertility. *J. Clin. Invest.* **103**, 11–18 (1999).
17. C. Bandi, T. J. Anderson, C. Genchi, M. L. Blaxter, Phylogeny of Wolbachia in filarial nematodes. *Proc. Biol. Sci.* **265**, 2407–2413 (1998).
18. M. J. Taylor, *Wolbachia* bacteria of filarial nematodes in the pathogenesis of disease and as a target for control. *Trans. R. Soc. Trop. Med. Hyg.* **94**, 596–598 (2000).
19. A. Hoerauf, Filariasis: New drugs and new opportunities for lymphatic filariasis and onchocerciasis. *Curr. Opin. Infect. Dis.* **21**, 673–681 (2008).
20. A. Hoerauf, S. Specht, M. Büttner, K. Pfarr, S. Mand, R. Fimmers, Y. Marfo-Debrekyei, P. Konadu, A. Y. Debrah, C. Bandi, N. Brattig, A. Albers, J. Larbi, L. Batsa, M. J. Taylor, O. Adjei, D. W. Buttner, *Wolbachia* endobacteria depletion by doxycycline as antifilarial therapy has macrofilaricidal activity in onchocerciasis: A randomized placebo-controlled study. *Med. Microbiol. Immunol.* **197**, 335 (2008).
21. M. J. Taylor, W. H. Makunde, H. F. McGarry, J. D. Turner, S. Mand, A. Hoerauf, Macrofilaricidal activity after doxycycline treatment of *Wuchereria bancrofti*: A double-blind, randomised placebo-controlled trial. *Lancet* **365**, 2116–2121 (2005).
22. M. Walker, S. Specht, T. S. Churcher, A. Hoerauf, M. J. Taylor, M. G. Basanez, Therapeutic efficacy and macrofilaricidal activity of doxycycline for the treatment of river blindness. *Clin. Infect. Dis.* **60**, 1199–1207 (2015).
23. J. D. Turner, S. Mand, A. Y. Debrah, J. Muehlfeld, K. Pfarr, H. F. McGarry, O. Adjei, M. J. Taylor, A. Hoerauf, A randomized, double-blind clinical trial of a 3-week course of doxycycline plus albendazole and ivermectin for the treatment of *Wuchereria bancrofti* infection. *Clin. Infect. Dis.* **42**, 1081–1089 (2006).
24. H. F. Cross, M. Haarbrink, G. Egerton, M. Yazdanbakhsh, M. J. Taylor, Severe reactions to filarial chemotherapy and release of Wolbachia endosymbionts into blood. *Lancet* **358**, 1873–1875 (2001).
25. L. R. Serbus, F. Landmann, W. M. Bray, P. M. White, J. Ruybal, R. S. Lokey, A. Debec, W. Sullivan, A cell-based screen reveals that the albendazole metabolite, albendazole sulfone, targets *Wolbachia*. *PLOS Pathog.* **8**, e1002922 (2012).
26. P. M. White, L. R. Serbus, A. Debec, A. Codina, W. Bray, A. Guichet, R. S. Lokey, W. Sullivan, Reliance of *Wolbachia* on high rates of host proteolysis revealed by a genome-wide RNAi screen of *Drosophila* cells. *Genetics* **205**, 1473–1488 (2017).
27. F. Fenollar, M. Maurin, D. Raoult, *Wolbachia pipientis* growth kinetics and susceptibilities to 13 antibiotics determined by immunofluorescence staining and real-time PCR. *Antimicrob. Agents Chemother.* **47**, 1665–1671 (2003).
28. P. G. Hermans, C. A. Hart, A. J. Trees, In vitro activity of antimicrobial agents against the endosymbiont *Wolbachia pipientis*. *J. Antimicrob. Chemother.* **47**, 659–663 (2001).
29. J. Janes, M. E. Young, E. Chen, N. H. Rogers, S. Burgstaller-Muehlbacher, L. D. Hughes, M. S. Love, M. V. Hull, K. L. Kuhen, A. K. Woods, S. B. Joseph, H. M. Petrassi, C. W. McNamara, M. S. Tremblay, A. I. Su, P. G. Schultz, A. K. Chatterjee, The ReFRAME library as a comprehensive drug repurposing library and its application to the treatment of cryptosporidiosis. *Proc. Natl. Acad. Sci. U.S.A.* **115**, 10750–10755 (2018).
30. V. Foray, M. M. Pérez-Jiménez, N. Fattouh, F. Landmann, *Wolbachia* control stem cell behavior and stimulate germline proliferation in filarial nematodes. *Dev. Cell* **45**, 198–211.e3 (2018).
31. G. S. Bah, E. L. Ward, A. Srivastava, A. J. Trees, V. N. Tanya, B. L. Makepeace, Efficacy of three-week oxytetracycline or rifampin monotherapy compared with a combination regimen against the filarial nematode *Onchocerca ochengi*. *Antimicrob. Agents Chemother.* **58**, 801–810 (2014).
32. V. Alagarsamy, K. Chitra, G. Saravanan, V. R. Solomon, M. T. Sulthana, B. Narendhar, An overview of quinazolines: Pharmacological significance and recent developments. *Eur. J. Med. Chem.* **151**, 628–685 (2018).
33. I. Khan, S. Zaib, S. Batool, N. Abbas, Z. Ashraf, J. Iqbal, A. Saeed, Quinazolines and quinazolinones as ubiquitous structural fragments in medicinal chemistry: An update on the development of synthetic methods and pharmacological diversification. *Bioorg. Med. Chem.* **24**, 2361–2381 (2016).
34. S. Specht, K. M. Pfarr, S. Arriens, M. P. Hübner, U. Klarmann-Schulz, M. Koschel, S. Sternberg, C. Martin, L. Ford, M. J. Taylor, A. Hoerauf, Combinations of registered drugs reduce treatment times required to deplete *Wolbachia* in the *Litomosoides sigmodontis* mouse model. *PLOS Negl. Trop. Dis.* **12**, e0006116 (2018).
35. M. Gerth, M. T. Gansauge, A. Weigert, C. Bleidorn, Phylogenomic analyses uncover origin and spread of the *Wolbachia* pandemic. *Nat. Commun.* **5**, 5117 (2014).
36. F. Comandatore, R. Cordaux, C. Bandi, M. Blaxter, A. Darby, B. L. Makepeace, M. Montagna, D. Sassera, Supergroup C *Wolbachia*, mutualist symbionts of filarial nematodes, have a distinct genome structure. *Open Biol.* **5**, 150099 (2015).
37. M. Blaxter, G. Koutsovoulos, The evolution of parasitism in Nematoda. *Parasitology* **142** (suppl. 1), S26–S39 (2015).
38. A. Halliday, A. F. Guimaraes, H. E. Tyrer, H. M. Metuge, C. N. Patrick, K. O. Arnaud, T. D. Kwenti, G. Forsbrook, A. Steven, D. Cook, P. Enyong, S. Wanji, M. J. Taylor, J. D. Turner, A murine macrofilaricide pre-clinical screening model for onchocerciasis and lymphatic filariasis. *Parasit. Vectors* **7**, 472 (2014).
39. R. Morales-Hojas, R. A. Cheke, R. J. Post, Molecular systematics of five *Onchocerca* species (Nematoda: Filarioidea) including the human parasite, *O. volvulus*, suggest sympatric speciation. *J. Helminthol.* **80**, 281–290 (2006).
40. K. L. Johnston, D. A. N. Cook, N. G. Berry, W. David Hong, R. H. Clare, M. Goddard, L. Ford, G. L. Nixon, P. M. O'Neill, S. A. Ward, M. J. Taylor, Identification and prioritization of novel anti-*Wolbachia* chemotypes from screening a 10,000-compound diversity library. *Sci. Adv.* **3**, eaao1551 (2017).
41. K. L. Johnston, L. Ford, I. Umareddy, S. Townson, S. Specht, K. Pfarr, A. Hoerauf, R. Altmeyer, M. J. Taylor, Repurposing of approved drugs from the human pharmacopoeia to target *Wolbachia* endosymbionts of onchocerciasis and lymphatic filariasis. *Int. J. Parasitol. Drugs Drug Resist.* **4**, 278–286 (2014).
42. R. H. Clare, D. A. Cook, K. L. Johnston, L. Ford, S. A. Ward, M. J. Taylor, Development and validation of a high-throughput anti-*Wolbachia* whole-cell screen: A route to macrofilaricidal drugs against onchocerciasis and lymphatic filariasis. *J. Biomol. Screen.* **20**, 64–69 (2015).
43. J. Foster, M. Ganatra, I. Kamal, J. Ware, K. Makarova, N. Ivanova, A. Bhattacharyya, V. Kapatral, S. Kumar, J. Posfai, T. Vincze, J. Ingram, L. Moran, A. Lapidus, M. Omelchenko, N. Kyrpides, E. Ghedin, S. Wang, E. Goltsman, V. Joukov, O. Ostrovskaya, K. Tsukerman, M. Mazur, D. Comb, E. Koonin, B. Slatko, The *Wolbachia* genome of *Brugia malayi*: Endosymbiont evolution within a human pathogenic nematode. *PLOS Biol.* **3**, e121 (2005).
44. A. Muslim, M. Y. Fong, R. Mahmud, S. Sivanandam, Vector and reservoir host of a case of human *Brugia pahangi* infection in Selangor, peninsular Malaysia. *Trop. Biomed.* **30**, 727–730 (2013).
45. Y. L. Lau, W. C. Lee, J. Xia, G. Zhang, R. Razali, A. Anwar, M. Y. Fong, Draft genome of *Brugia pahangi*: High similarity between *B. pahangi* and *B. malayi*. *Parasit. Vectors* **8**, 451 (2015).
46. J. C. Molloy, U. Sommer, M. R. Viant, S. P. Sinkins, *Wolbachia* modulates lipid metabolism in *Aedes albopictus* mosquito cells. *Appl. Environ. Microbiol.* **82**, 3109–3120 (2016).
47. L. R. Serbus, P. M. White, J. P. Silva, A. Rabe, L. Teixeira, R. Albertson, W. Sullivan, The impact of host diet on *Wolbachia* titer in *Drosophila*. *PLOS Pathog.* **11**, e1004777 (2015).
48. T. Ikeya, S. Broughton, N. Alic, R. Grandison, L. Partridge, The endosymbiont *Wolbachia* increases insulin/IGF-like signalling in *Drosophila*. *Proc. Biol. Sci.* **276**, 3799–3807 (2009).
49. R. T. Jacobs, C. Lunde, Y. R. Freund, V. Hernandez, X. Li, Y. Xia, P. W. Berry, J. Halladay, R. Stefanakis, E. E. Easom, J. J. Plattner, L. Ford, K. L. Johnston, D. A. N. Cook, R. Clare, A. Cassidy, L. Myhill, H. Tyrer, G. Gamble, A. F. Guimaraes, A. Steven, F. Lenz, A. Ehrens, S. J. Frohberger, M. Koschel, A. Hoerauf, M. P. Hübner, C. McNamara, M. A. Bakowski, J. D. Turner, M. J. Taylor, S. A. Ward, Boron-pleuromutilins as anti-*Wolbachia* agents with potential for treatment of onchocerciasis and lymphatic filariasis. *J. Med. Chem.* **62**, 2521–2540 (2018).
50. M. J. Taylor, T. W. von Geldern, L. Ford, M. P. Hubner, K. Marsh, K. L. Johnston, H. T. Sjoberg, S. Specht, N. Pionnier, H. E. Tyrer, R. H. Clare, D. A. N. Cook, E. Murphy, A. Steven, J. Archer, D. Bloemker, F. Lenz, M. Koschel, A. Ehrens, H. M. Metuge, V. C. Chunda, P. W. Ndongmo Chounna, A. J. Njouendou, F. F. Fombad, R. Carr, H. E. Morton, G. Aljayyoussi, A. Hoerauf, S. Wanji, D. J. Kempf, J. D. Turner, S. A. Ward, Preclinical development of an oral anti-*Wolbachia* macrolide drug for the treatment of lymphatic filariasis and onchocerciasis. *Sci. Transl. Med.* **11**, eaau2086 (2019).
51. C. P. Morris, H. Evans, S. E. Larsen, E. Mitre, A comprehensive, model-based review of vaccine and repeat infection trials for filariasis. *Clin. Microbiol. Rev.* **26**, 381–421 (2013).
52. J. Gilbert, C. K. Nfon, B. L. Makepeace, L. M. Njongmeta, I. M. Hastings, K. M. Pfarr, A. Renz, V. N. Tanya, A. J. Trees, Antibiotic chemotherapy of onchocerciasis: In a bovine model, killing of adult parasites requires a sustained depletion of endosymbiotic bacteria (*Wolbachia* species). *J. Infect. Dis.* **192**, 1483–1493 (2005).

53. W. D. Hong, F. Benayoud, G. L. Nixon, L. Ford, K. L. Johnston, R. H. Clare, A. Cassidy, D. A. N. Cook, A. Siu, M. Shiotani, P. J. H. Webborn, S. Kavanagh, G. Aljayyoussi, E. Murphy, A. Steven, J. Archer, D. Struever, S. J. Frohberger, A. Ehrens, M. P. Hubner, A. Hoerauf, A. P. Roberts, A. T. M. Hubbard, E. W. Tate, R. A. Serwa, S. C. Leung, L. Qie, N. G. Berry, F. Gusovsky, J. Hemingway, J. D. Turner, M. J. Taylor, S. A. Ward, P. M. O'Neill, AWZ1066S, a highly specific anti-*Wolbachia* drug candidate for a short-course treatment of filariasis. *Proc. Natl. Acad. Sci. U.S.A.* **116**, 1414–1419 (2019).
54. A. Heddi, A. M. Grenier, C. Khatchadourian, H. Charles, P. Nardon, Four intracellular genomes direct weevil biology: Nuclear, mitochondrial, principal endosymbiont, and *Wolbachia*. *Proc. Natl. Acad. Sci. U.S.A.* **96**, 6814–6819 (1999).
55. B. M. Fuchs, G. Wallner, W. Beisker, I. Schwippl, W. Ludwig, R. Amann, Flow cytometric analysis of the in situ accessibility of *Escherichia coli* 16S rRNA for fluorescently labeled oligonucleotide probes. *Appl. Environ. Microbiol.* **64**, 4973–4982 (1998).
56. M. A. Perotti, H. K. Clarke, B. D. Turner, H. R. Braig, Rickettsia as obligate and mycetomic bacteria. *FASEB J.* **20**, 2372–2374 (2006).
57. T. Koressaar, M. Remm, Enhancements and modifications of primer design program Primer3. *Bioinformatics* **23**, 1289–1291 (2007).
58. A. Untergasser, I. Cutcutache, T. Koressaar, J. Ye, B. C. Faircloth, M. Remm, S. G. Rozen, Primer3—New capabilities and interfaces. *Nucleic Acids Res.* **40**, e115 (2012).
59. B. W. Li, Z. Wang, A. C. Rush, M. Mitreva, G. J. Weil, Transcription profiling reveals stage- and function-dependent expression patterns in the filarial nematode *Brugia malayi*. *BMC Genomics* **13**, 184 (2012).
60. M. W. Pfaffl, A new mathematical model for relative quantification in real-time RT-PCR. *Nucleic Acids Res.* **29**, e45 (2001).
61. L. Volkmann, O. Bain, M. Saeftel, S. Specht, K. Fischer, F. Brombacher, K. I. Matthaei, A. Hoerauf, Murine filariasis: Interleukin 4 and interleukin 5 lead to containment of different worm developmental stages. *Med. Microbiol. Immunol.* **192**, 23–31 (2003).
62. J. D. Turner, R. Sharma, G. Al Jayoussi, H. E. Tyrer, J. Gamble, L. Hayward, R. S. Priestley, E. A. Murphy, J. Davies, D. Waterhouse, D. A. N. Cook, R. H. Clare, A. Cassidy, A. Steven, K. L. Johnston, J. McCall, L. Ford, J. Hemingway, S. A. Ward, M. J. Taylor, Albendazole and antibiotics synergize to deliver short-course anti-*Wolbachia* curative treatments in preclinical models of filariasis. *Proc. Natl. Acad. Sci. U.S.A.* **114**, E9712–E9721 (2017).
63. D. Zofou, F. F. Fombad, N. V. T. Gandjui, A. J. Njouendou, A. J. Kengne-Ouafo, P. W. Chounna Ndongmo, F. R. Datchoua-Poutcheu, P. A. Enyong, D. T. Bita, M. J. Taylor, J. D. Turner, S. Wanji, Evaluation of *in vitro* culture systems for the maintenance of microfilariae and infective larvae of *Loa loa*. *Parasit. Vectors* **11**, 275 (2018).
64. S. Wanji, E. E. Eyong, N. Tendongfor, C. Ngwa, E. Esuka, A. Kengne-Ouafo, F. Datchoua-Poutcheu, P. Enyong, A. Hopkins, C. D. Mackenzie, Parasitological, hematological and biochemical characteristics of a model of hyper-microfilariaemic loiasis (*Loa loa*) in the Baboon (*Papio anubis*). *PLOS Negl. Trop. Dis.* **9**, e0004202 (2015).
65. O. A. Fahmi, J. L. Raucy, E. Ponce, S. Hassanali, J. M. Lasker, Utility of DPX2 cells for predicting CYP3A induction-mediated drug-drug interactions and associated structure-activity relationships. *Drug Metab. Dispos.* **40**, 2204–2211 (2012).
66. J. Bowes, A. J. Brown, J. Hamon, W. Jarolimek, A. Sridhar, G. Waldron, S. Whitebread, Reducing safety-related drug attrition: The use of in vitro pharmacological profiling. *Nat. Rev. Drug Discov.* **11**, 909–922 (2012).
67. A. Schiefer, A. Schmitz, T. F. Schäberle, S. Specht, C. Lämmer, K. L. Johnston, D. G. Vassylyev, G. M. König, A. Hoerauf, K. Pfarr, Corallopyronin A specifically targets and depletes essential obligate *Wolbachia* endobacteria from filarial nematodes in vivo. *J. Infect. Dis.* **206**, 249–257 (2012).

Acknowledgments: We are grateful to Calibr's Compound Management and High-Throughput Screening groups for assistance with the project and to the members and leadership of the Macrofilaricide Drug Accelerator, especially K. Duncan, R. Elliott, and S. Mills. We thank M. Koschel, I. Johannes, M. Fendler, and V. Nikolov for technical support. We thank R. Wada for pharmacological assistance and expertise. **Funding:** This work was supported by grants from the Bill & Melinda Gates Foundation: no. OPP1107194 to Calibr, no. OPP1152825 to GHDDI, no. OPP1134310 to Bonn University, and no. OPP1119043 to J.D.T., S.W., and M.J.T.
Author contributions: M.S.T. and P.G.S. conceived the project. M.A.B., K.G., P.M.W., L.C., A.D., F. Landmann, W.S., and C.W.M. designed in vitro and ex vivo experiments. M.A.B. performed in vitro and ex vivo experiments. H.G. and M.A.B. performed bacterial panel experiments. M.P.H. and A.H. designed in vivo experiments using *L. sigmodontis*. B.D., S.J.F., A.E., D.S., F. Lenz, and M.P.H. performed in vivo experiments using *L. sigmodontis*. N.P., J.D.T., S.W., and M.J.T. designed in vivo experiments in SCID mice. N.P., E.M., J.A., A.S., V.C.C., F.F.F., P.W.C., A.J.N., H.M.M., B.L.N., N.V.G., D.N.A., and T.D.B.K. performed the in vivo experiments in SCID mice. R.K.S., R.L., J.O., B.Y., A.K.C., J.R., X.-J.C., and H.M.P. designed and performed synthesis and optimization. A.K.W. and S.B.J. coordinated preclinical profiling and pharmacokinetic studies. M.V.H. coordinated the high-throughput and compound management groups. W.X. and K.L.K. outlined the project workflow. M.A.B. wrote the manuscript. All authors edited the manuscript. **Competing interests:** The authors declare that they have no competing interests. **Data and materials availability:** All data associated with this study are present in the paper or the Supplementary Materials. Results from the primary in vitro screen of the ReFRAME library have been deposited to the reframedb.org data portal.

Submitted 13 October 2018
Accepted 18 March 2019
Published 8 May 2019
10.1126/scitranslmed.aav3523

Citation: M. A. Bakowski, R. K. Shiroodi, R. Liu, J. Olejniczak, B. Yang, K. Gagaring, H. Guo, P. M. White, L. Chappell, A. Debec, F. Landmann, B. Dubben, F. Lenz, D. Struever, A. Ehrens, S. J. Frohberger, H. Sjoberg, N. Pionnier, E. Murphy, J. Archer, A. Steven, V. C. Chunda, F. F. Fombad, P. W. Chounna, A. J. Njouendou, H. M. Metuge, B. L. Ndzeshang, N. V. Gandjui, D. N. Akumtoh, T. D. B. Kwenti, A. K. Woods, S. B. Joseph, M. V. Hull, W. Xiong, K. L. Kuhen, M. J. Taylor, S. Wanji, J. D. Turner, M. P. Hübner, A. Hoerauf, A. K. Chatterjee, J. Roland, M. S. Tremblay, P. G. Schultz, W. Sullivan, X.-J. Chu, H. M. Petrassi, C. W. McNamara, Discovery of short-course antiwolbachial quinazolines for elimination of filarial worm infections. *Sci. Transl. Med.* **11**, eaav3523 (2019).

Science Translational Medicine

Discovery of short-course antiwolbachial quinazolines for elimination of filarial worm infections

Malina A. Bakowski, Roohollah Kazem Shiroodi, Renhe Liu, Jason Olejniczak, Baiyuan Yang, Kerstin Gagaring, Hui Guo, Pamela M. White, Laura Chappell, Alain Debec, Frédéric Landmann, Bettina Dubben, Franziska Lenz, Dominique Struever, Alexandra Ehrens, Stefan J. Frohberger, Hanna Sjoberg, Nicolas Pionnier, Emma Murphy, John Archer, Andrew Steven, Valerine C. Chunda, Fanny F. Fombad, Patrick W. Chounna, Abdel J. Njouendou, Haelly M. Metuge, Bertrand L. Ndzeshang, Narcisse V. Gandjui, Desmond N. Akumtoh, Tayong D. B. Kwenti, Ashley K. Woods, Sean B. Joseph, Mitchell V. Hull, Wen Xiong, Kelli L. Kuhen, Mark J. Taylor, Samuel Wanji, Joseph D. Turner, Marc P. Hübner, Achim Hoerauf, Arnab K. Chatterjee, Jason Roland, Matt S. Tremblay, Peter G. Schultz, William Sullivan, Xin-Jie Chu, H. Michael Petrassi and Case W. McNamara

Sci Transl Med **11**, eaav3523.
DOI: 10.1126/scitranslmed.aav3523

Walloping Wolbachia with quinazolines

A variety of adult parasitic worms depend on the bacterial endosymbiont *Wolbachia* for reproduction and survival, so *Wolbachia* is a clinical target for treating filarial nematodes. Antibiotics effective against *Wolbachia* require weeks of treatment and are not suitable for all patients. Bakowski *et al.* therefore performed a high-throughput phenotypic screen to look for alternative antiwolbachial compounds, which led them to quinazolines. Lead compounds were optimized and showed efficacy in multiple mouse filarial models, performing well or even better than 2 weeks of antibiotics. Their results suggest that a short course of quinazolines could eradicate *Wolbachia*, potentially eliminating adult worms in infected humans.